PHYSICAL REVIEW B VOLUME 39, NUMBER 8 15 MARCH 1989-I

Mobility, interdiffusion, and tracer diffusion in lattice-gas models of two-component alloys

K. W. Kehr
Institut für Festkörperforschung der Kernforschungsanlage Jülich, Postfach 1913, D-5170 Jülich, Federal Republic of Germany

K. Binder
Institut für Physik, Universität Mainz, Postfach 3980, D-6500 Mainz, Federal Republic of Germany

S. M. Reulein
Institut für Festkörperforschung der Kernforschungsanlage Jülich, Postfach 1913, D-5170 Jülich, Federal Republic of Germany
(Received 18 July 1988)

The transport properties of lattice-gas models of alloys with two particle species are studied. The numbers of the particles and vacancies are conserved, and the two particle species have different exchange rates with the vacancies. The mobility and interdiffusion is described by the linear Onsager theory of transport. The Onsager coefficients are estimated from numerical simulations of the mobilities. A recently proposed relation between the Onsager coefficients of the random-alloy model is verified. The interdiffusion of the two species is directly monitored in the simulations; it is well described by the estimated Onsager coefficients. The results on interdiffusion are compared with simulation results on tracer diffusion. The interdiffusion cannot be expressed by the average, or the inverse average, of the tracer-diffusion coefficients. An exception is the case of identical transition rates where the interdiffusion coefficient is given by the tracer-diffusion coefficient.

I. INTRODUCTION

In this paper we investigate the interdiffusion in lattice-gas models of two species of particles with different transition rates. Interdiffusion is a common phenomenon in metal physics. Many investigations were done of interdiffusion of one species of metal atoms into another, and also of the interdiffusion in random alloys. Reviews of the theoretical concepts, together with references of experimental work, can be found in Refs. 1–3. Interdiffusion has also been studied experimentally and theoretically for polymer mixtures (for a short review, see Ref. 4). A central question in both fields is how the process of interdiffusion is related to simpler physical quantities, for instance, self-diffusion coefficients of the individual species. In this context some controversy arose in the field of polymers.

We decided to investigate interdiffusion of two species of particles in lattice-gas models, since they are well-defined models, where the theory can be developed explicitly to some extent, and, second, since they are easily amenable to numerical simulations. Of course, these models contain simplifying features compared to real systems. For instance, the creation and destruction of vacancies at imperfections makes important contributions to the diffusion properties of mixtures of metals. Such processes are difficult to incorporate into the theory or into simulations and we omitted them completely.

We describe interdiffusion and self-diffusion in the lattice-gas models in terms of the Onsager formulation of linearized nonequilibrium thermodynamics. The necessary thermodynamic functions are obtained from the statistics of the lattice gases. This is done in Sec. II. Our aim is an unambiguous formulation of the interdiffusion process, which in our opinion can be achieved for these well-defined models. The Onsager coefficients which are undetermined parameters in the formulations of Sec. II are determined from numerical simulations in Sec. III. Here we explore various ratios of the transition rates and the concentrations of the particle species. The exactly known case of equal transition rates is verified; other limiting cases are also easily understood, as will be discussed in this section. The Onsager coefficients are then used to evaluate explicitly the interdiffusion process in Sec. IV. The results are compared with direct numerical simulations of the interdiffusion process, where the decay of concentration profiles is monitored. It turns out that a complete description of the interdiffusion process is achieved, within the accuracy of the numerical simulations. The problem of possible relations of interdiffusion with self-diffusion is taken up in Sec. V. The tracer-diffusion coefficients of both particle species are determined by numerical simulations and compared with the Onsager formulation of self-diffusion and with controversial propositions for their relation with interdiffusion. Section VI first summarizes the conclusions of our study of interdiffusion in lattice-gas models. Thereafter the connection and also the differences to interdiffusion in metal alloys and polymers are discussed.

II. ONSAGER DESCRIPTION OF INTERDIFFUSION

A. Thermodynamics of lattice-gas models

In this section we will describe interdiffusion of lattice-gas particles in the frame of Onsager's linearized

nonequilibrium transport theory. The thermodynamics of lattice gases is required as an ingredient and developed in this section. We consider a lattice with N sites, occupied with N_A particles of species A, N_B particles of species B, and N_V vacancies. For comparison with related work we treat vacancies in this section as a separate, independent species. We consider N_A, N_B, and N_V as variable quantities (alternatively we could regard the number N of sites as varying). Of course, $N=N_A+N_B+N_V$. It is expedient to introduce the fractional occupancies

$$\phi_A=\frac{N_A}{N},\quad \phi_B=\frac{N_B}{N},\quad \phi_V=\frac{N_V}{N}\ , \tag{2.1a}$$

where

$$\phi_A+\phi_B+\phi_V=1\ . \tag{2.1b}$$

To give a specific form of the free energy F of the lattice-gas model we assume a mean-field-type interaction of the particles, or, equivalently, we utilize the Bragg-Williams approximation,

$$\begin{aligned}F=k_BT\Big[&N_A\ln N_A+N_B\ln N_B+N_V\ln N_V-N\ln N\\&+\chi_{AA}\frac{N_A^2}{2N}+\chi_{BB}\frac{N_B^2}{2N}+\chi_{VV}\frac{N_V^2}{2N}\\&+\chi_{AB}\frac{N_AN_B}{N}+\chi_{AV}\frac{N_AN_V}{N}+\chi_{BV}\frac{N_BN_V}{N}\Big]\ .\end{aligned} \tag{2.2}$$

The coefficients χ_{ij} specify the interactions of the different species of particles and vacancies. A modification in the entropy term is necessary if polymer chains of lengths n_A, n_B are considered; this possibility will be disregarded. The free energy per lattice site $f=F/N$ is then given by

$$\begin{aligned}f=k_BT(&\phi_A\ln\phi_A+\phi_B\ln\phi_B+\phi_V\ln\phi_V\\&+\tfrac{1}{2}\chi_{AA}\phi_A^2+\tfrac{1}{2}\chi_{BB}\phi_B^2+\tfrac{1}{2}\chi_{VV}\phi_V^2\\&+\chi_{AB}\phi_A\phi_B+\chi_{AV}\phi_A\phi_V+\chi_{BV}\phi_B\phi_V)\ .\end{aligned} \tag{2.3}$$

The chemical potentials of the different species are obtained from the standard definition

$$\mu_i=\left(\frac{\partial F}{\partial N_i}\right)_{T,N_{j\,(\neq i)}}\ . \tag{2.4}$$

Using $F=Nf$ and differentiating with respect to the ϕ_i we have

$$\mu_i=f+\sum_j\frac{\partial f}{\partial\phi_j}(\delta_{ij}-\phi_j)\ , \tag{2.5}$$

where the sum runs over A, B, and V. The chemical potentials are given explicitly by

$$\begin{aligned}\beta\mu_A=\beta f&+(1-\phi_A)(\ln\phi_A+1+\chi_{AA}\phi_A+\chi_{AB}\phi_B+\chi_{AV}\phi_V)\\&-\phi_B(\ln\phi_B+1+\chi_{AB}\phi_A+\chi_{BB}\phi_B+\chi_{BV}\phi_V)\\&-\phi_V(\ln\phi_V+1+\chi_{AV}\phi_A+\chi_{BV}\phi_B+\chi_{VV}\phi_V)\ ,\end{aligned} \tag{2.6a}$$

$$\begin{aligned}\beta\mu_B=\beta f&-\phi_A(\ln\phi_A+1+\chi_{AA}\phi_A+\chi_{AB}\phi_B+\chi_{AV}\phi_V)\\&+(1-\phi_B)(\ln\phi_B+1+\chi_{AB}\phi_A+\chi_{BB}\phi_B+\chi_{BV}\phi_V)\\&-\phi_V(\ln\phi_V+1+\chi_{AV}\phi_A+\chi_{BV}\phi_B+\chi_{VV}\phi_V)\ ,\end{aligned} \tag{2.6b}$$

$$\begin{aligned}\beta\mu_V=\beta f&-\phi_A(\ln\phi_A+1+\chi_{AA}\phi_A+\chi_{AB}\phi_B+\chi_{AV}\phi_V)\\&-\phi_B(\ln\phi_B+1+\chi_{AB}\phi_A+\chi_{BB}\phi_B+\chi_{BV}\phi_V)\\&+(1-\phi_V)(\ln\phi_V+1+\chi_{AV}\phi_A+\chi_{BV}\phi_B+\chi_{VV}\phi_V)\ ,\end{aligned} \tag{2.6c}$$

where $\beta=(k_BT)^{-1}$. Note that three chemical potentials appear, since we consider N_A, N_B, and N_V as varying quantities. However, they are related to each other by the Duhem-Gibbs relation.

The Duhem-Gibbs relation is a consequence of the extensivity of the energy as a function of extensive variables. We have

$$dF=-S\,dT+\sum_i\mu_i\,dN_i\ , \tag{2.7}$$

where S is the entropy. Introducing the energy $E=F+TS$ we obtain

$$dE=T\,dS+\sum_i\mu_i\,dN_i \tag{2.8}$$

and, since E must be a homogeneous function of degree 1 of the extensive variables,

$$E=TS+\sum_i\mu_iN_i\ , \tag{2.9}$$

or, equivalently,

$$f=\mu_A\phi_A+\mu_B\phi_B+\mu_V\phi_V\ . \tag{2.10}$$

This last relation is easily verified from Eq. (2.5).

We did not specify the volume or the pressure in our derivations. There is no need to do so in the lattice-gas models, but one may include one of these variables.

Comparison of the differential

$$df=-s\,dT+\sum_i\frac{\partial f}{\partial\phi_i}d\phi_i \tag{2.11}$$

with the explicit differential of (2.10) and use of (2.5) establishes the Duhem-Gibbs relation in the form, valid for isothermal processes ($dT=0$):

$$\phi_A\,d\mu_A+\phi_B\,d\mu_B+\phi_V\,d\mu_V=0\ . \tag{2.12}$$

It is frequently assumed in metal physics and also in polymer physics that μ_V is identically zero. This leads to a reduced form of the Duhem-Gibbs relation. The use of $\mu_V\equiv0$ is justified in these articles by the assumption of a

"local equilibrium" of the vacancies. We will comment on this assumption in Sec. VI. In our work we will not make this assumption, i.e., μ_V will be explicitly taken into account. Although we will not use (2.12) explicitly, it will be fulfilled in our derivations.

B. Onsager formalism

We now consider nonequilibrium situations, characterized by gradients of chemical potentials and particle densities, which lead to particle currents. We assume that a hydrodynamic description is possible, i.e., that local thermodynamic equilibrium exists. In the usual way the global variables ϕ_i are replaced by space- and time-dependent local variables, which we call concentrations,

$$\phi_A \rightarrow c_A(\mathbf{r},t), \quad \phi_B \rightarrow c_B(\mathbf{r},t), \quad \phi_V \rightarrow c_V(\mathbf{r},t) .$$

We have locally, at each instant of time,

$$c_A(\mathbf{r},t)+c_B(\mathbf{r},t)+c_V(\mathbf{r},t)=1 . \tag{2.13}$$

We assume now that the particle and vacancy numbers N_A, N_B, and N_V are conserved. These conservation laws lead locally to the continuity equations

$$\frac{\partial c_A}{\partial t}+\nabla\cdot\mathbf{j}_A=0, \quad \frac{\partial c_B}{\partial t}+\nabla\cdot\mathbf{j}_B=0, \quad \frac{\partial c_V}{\partial t}+\nabla\cdot\mathbf{j}_V=0 . \tag{2.14}$$

The current densities $\mathbf{j}_i$ have dimensions of velocities. They could be redefined by introducing the volume per lattice site, but this is not done here. From (2.13) we find

$$\nabla\cdot(\mathbf{j}_A+\mathbf{j}_B+\mathbf{j}_V)=0 , \tag{2.15a}$$

and since we will not admit uniform or rotational flow patterns,

$$\mathbf{j}_A+\mathbf{j}_B+\mathbf{j}_V=\mathbf{0} . \tag{2.15b}$$

The constitutive linear equations relating the current densities to the gradients of the chemical potentials are

$$\mathbf{j}_A=-\beta\Lambda_{AA}\nabla\mu_A-\beta\Lambda_{AB}\nabla\mu_B-\beta\Lambda_{AV}\nabla\mu_V , \tag{2.16a}$$

$$\mathbf{j}_B=-\beta\Lambda_{BA}\nabla\mu_A-\beta\Lambda_{BB}\nabla\mu_B-\beta\Lambda_{BV}\nabla\mu_V , \tag{2.16b}$$

$$\mathbf{j}_V=-\beta\Lambda_{VA}\nabla\mu_A-\beta\Lambda_{VB}\nabla\mu_B-\beta\Lambda_{VV}\nabla\mu_V . \tag{2.16c}$$

These equations define the Onsager coefficients Λ_{ij}. For simplicity we have assumed isothermal processes, i.e., no temperature gradients are allowed. Also, external forces have been omitted in (2.16); they will be introduced in the following section. The Onsager symmetry relations require

$$\Lambda_{AB}=\Lambda_{BA}, \quad \Lambda_{AV}=\Lambda_{VA}, \quad \Lambda_{BV}=\Lambda_{VB} . \tag{2.17}$$

The condition (2.15b) of vanishing total current yields a further condition,

$$(\Lambda_{AA}+\Lambda_{BA}+\Lambda_{VA})\nabla\mu_A+(\Lambda_{AB}+\Lambda_{BB}+\Lambda_{VB})\nabla\mu_B +(\Lambda_{AV}+\Lambda_{BV}+\Lambda_{VV})\nabla\mu_V=0 . \tag{2.18}$$

In order that this condition be fulfilled for arbitrary μ_A, μ_B, and μ_V, we must require [although the μ_i are related by the Duhem-Gibbs relation, the condition (2.18) is completely independent of it]

$$\begin{aligned}&\Lambda_{AA}+\Lambda_{BA}+\Lambda_{VA}=0 ,\\ &\Lambda_{AB}+\Lambda_{BB}+\Lambda_{VB}=0 ,\\ &\Lambda_{AV}+\Lambda_{BV}+\Lambda_{VV}=0 .\end{aligned} \tag{2.19}$$

These relations allow the elimination of all Onsager coefficients that involve the vacancies

$$\begin{aligned}&\Lambda_{VA}=-(\Lambda_{AA}+\Lambda_{BA}) ,\\ &\Lambda_{VB}=-(\Lambda_{AB}+\Lambda_{BB}) ,\\ &\Lambda_{VV}=\Lambda_{AA}+2\Lambda_{AB}+\Lambda_{BB} .\end{aligned} \tag{2.20}$$

Using these relations the particle current densities $\mathbf{j}_A$ and $\mathbf{j}_B$ can be expressed in the following form:

$$\begin{aligned}&\mathbf{j}_A=-\beta\Lambda_{AA}\nabla(\mu_A-\mu_V)-\beta\Lambda_{AB}\nabla(\mu_B-\mu_V) ,\\ &\mathbf{j}_B=-\beta\Lambda_{BA}\nabla(\mu_A-\mu_V)-\beta\Lambda_{BB}\nabla(\mu_B-\mu_V) .\end{aligned} \tag{2.21}$$

Note that only the differences $\mu_A-\mu_V$ and $\mu_B-\mu_V$ appear. The form of Eqs. (2.21) is essentially a consequence of particle-number conservation, as is evident from their derivation.

The next step is to relate gradients of chemical potentials to gradients of particle concentrations. This can be achieved, for instance, by using the chemical potentials derived within the mean-field approximation in Sec. II A. The μ_i are given by Eq. (2.6) where the ϕ_i should be substituted by $c_i(\mathbf{r},t)$. We obtain

$$\begin{aligned}\beta\nabla(\mu_A-\mu_V)=&\left[\frac{1}{c_A}+\chi_{AA}\right]\nabla c_A+\chi_{AB}\nabla c_B+\chi_{AV}\nabla c_V\\ &-\left[\chi_{AV}\nabla c_A+\chi_{BV}\nabla c_B+\left[\frac{1}{c_V}+\chi_{VV}\right]\nabla c_V\right] ,\\ \beta\nabla(\mu_B-\mu_V)=&\chi_{AB}\nabla c_A+\left[\frac{1}{c_B}+\chi_{BB}\right]\nabla c_B+\chi_{BV}\nabla c_V\\ &-\left[\chi_{AV}\nabla c_A+\chi_{BV}\nabla c_B+\left[\frac{1}{c_V}+\chi_{VV}\right]\nabla c_V\right] .\end{aligned} \tag{2.22}$$

The concentrations c_i in the large parentheses should be replaced by their global values ϕ_i, in accordance with the *linear* theory of transport. From now on we use c_i both for the local and global variables; the meaning will be clear from the context.

It remains to eliminate the gradient of the vacancy concentration by using $\nabla c_V=-\nabla(c_A+c_B)$. We can then give the linear relations between current densities and gradients of particle densities. While we have used Latin indices for the three components A, B, and V, we now use Greek indices for the two species A and B. We have

$$\mathbf{j}_\alpha = -\sum_{\beta=A,B} D_{\alpha\beta}\nabla c_\beta \ , \tag{2.23}$$

where the elements of the diffusivity matrix are given by

$$\begin{aligned}
D_{AA} &= \Lambda_{AA}\left[\frac{1}{c_A}+\frac{1}{c_V}+\chi_{AA}+\chi_{VV}-2\chi_{AV}\right] \\
&\quad +\Lambda_{AB}\left[\frac{1}{c_V}+\chi_{AB}+\chi_{VV}-\chi_{AV}-\chi_{BV}\right], \\
D_{AB} &= \Lambda_{AA}\left[\frac{1}{c_V}+\chi_{AB}+\chi_{VV}-\chi_{AV}-\chi_{BV}\right] \\
&\quad +\Lambda_{AB}\left[\frac{1}{c_B}+\frac{1}{c_V}+\chi_{BB}+\chi_{VV}-2\chi_{BV}\right], \\
D_{BA} &= \Lambda_{AB}\left[\frac{1}{c_A}+\frac{1}{c_V}+\chi_{AA}+\chi_{VV}-2\chi_{AV}\right] \\
&\quad +\Lambda_{BB}\left[\frac{1}{c_V}+\chi_{AB}+\chi_{VV}-\chi_{AV}-\chi_{BV}\right], \\
D_{BB} &= \Lambda_{AB}\left[\frac{1}{c_V}+\chi_{AB}+\chi_{VV}-\chi_{AV}-\chi_{BV}\right] \\
&\quad +\Lambda_{BB}\left[\frac{1}{c_B}+\frac{1}{c_V}+\chi_{BB}+\chi_{VV}-2\chi_{BV}\right].
\end{aligned} \tag{2.24}$$

Note that the matrix $D_{\alpha\beta}$ is no longer symmetric, contrary to $\Lambda_{\alpha\beta}$, but it is diagonalizable.

Although (2.24) is given in the Bragg-Williams approximation, the result is more general, if the coefficients χ are identified with appropriate second derivatives of the free energy per site.

Finally we combine the linear current relations with the continuity equations for the particle species to obtain a generalization of the diffusion equation,

$$\frac{\partial c_\alpha}{\partial t} = \sum_\beta D_{\alpha\beta}\nabla^2 c_\beta \ . \tag{2.25}$$

The concentration dependence of $D_{\alpha\beta}$ would entail an additional term on the right-hand side of (2.25). However, Eq. (2.25) is valid for linear deviations of the concentrations c_α from their equilibrium values.

We point out that once the set of three Onsager coefficients $\Lambda_{\alpha\beta}$ is known, and the equilibrium free energy per site, then the diffusion matrix entering Eq. (2.25) is completely specified. The further evaluation of (2.25) will be deferred to Sec. IV. It will be shown in that section that (2.25), together with appropriate boundary conditions, provides a complete description of interdiffusion in the lattice-gas models under consideration.

We close this section with a remark on the literature of this subject. The Onsager formulation of particle transport in fluids and solids has been considered in many articles; also questions such as the correct choices of the reference frames were frequently discussed. In most of the work the assumption that the vacancy concentration is regulated by the equilibrium condition $\mu_V \equiv 0$ is made at an early stage (see, for instance, Refs. 1–3). One exception is the formulation of multicomponent diffusion in crystals in Ref. 5. To avoid confusion we preferred to develop the appropriate Onsager description of transport for our lattice-gas models with conserved numbers of vacancies without reference to previous formulations.

III. DETERMINATION OF THE ONSAGER COEFFICIENTS

A. Simulation procedure

The Onsager coefficients of the lattice-gas model with two species of particles are not known exactly except for the case of identical transition rates of both species. Hence we estimate the Onsager coefficients of the model by numerical simulations for various concentrations and ratios of the transition rates, in two and three dimensions. Up to now the dynamics of the model was not clearly specified. In fact, the phenomenological Onsager formulation of Sec. II does not require such a specification. The dynamics that we use is exchange of vacancies with both particle species. The transition rate of an A particle to a vacant site shall be Γ_A, and that of a B particle Γ_B. Direct exchange of the particles is excluded; hence the model is relevant to metal and polymer physics. Further, all interactions between the particles are neglected, except the exclusion of double occupancy of lattice sites. Following the usual terminology we call this model *noninteracting*. Also the designation *random-alloy model* is commonly used.

We assume a uniform force in one direction imposed on one species of particles. Such a force is easily implemented in numerical simulations by introducing a bias of the transition rates of this species in one direction. When external forces $\mathbf{F}_j$ act on the particles of species j, the linear relations (2.16) between driving forces and current densities are extended to

$$\mathbf{j}_i = -\sum_j \beta\Lambda_{ij}(\nabla\mu_j - \mathbf{F}_j) \ . \tag{3.1}$$

The sum runs over A, B, and V and isothermal conditions are assumed. We do not consider any external forces acting on the vacancies. Thus we may eliminate the Onsager coefficients related to vacancies as in Sec. II. Also, we assume vanishing gradients of the chemical potential, equivalent to the absence of concentration gradients. The constitutive relations are then simply

$$\mathbf{j}_\alpha = \sum_\gamma \Lambda_{\alpha\gamma}\beta\mathbf{F}_\gamma \tag{3.2a}$$

or

$$\mathbf{v}_\alpha = \sum_\gamma \frac{1}{c_\alpha}\Lambda_{\alpha\gamma}\beta\mathbf{F}_\gamma \ , \tag{3.2b}$$

where the sum runs over A and B and $\mathbf{v}_\alpha$ is the velocity of species α. The force on one species of particles, say γ, is implemented by taking the transition rates in the x direction as

$$\Gamma_x^{(\gamma)} = b\Gamma_\gamma, \quad \Gamma_{-x}^{(\gamma)} = b^{-1}\Gamma_\gamma \tag{3.3}$$

with $b > 1$. The transition rates in all other directions are Γ_γ. To circumvent the (practical) problem of explicitly determining the force, we consider the drift of a single particle in an otherwise empty lattice. Its transition rates in the x direction are $\Gamma_x = b\Gamma$, $\Gamma_{-x} = b^{-1}\Gamma$, and in the other directions Γ. Its mean velocity in the x direction is

$$v_x^{\text{s.p.}} = \Gamma(b - b^{-1}) \ . \tag{3.4}$$

In the *linear* regime,

$$v_x^{\text{s.p.}} = \Gamma\beta F_x \ . \tag{3.5}$$

This expression follows from the Onsager coefficient of one species of noninteracting particles, $\Lambda = c(1-c)\Gamma$, in the limit $c \to 0$. Hence we have

$$\frac{v_x^{(\alpha)}}{v_x^{\text{s.p.}}} = \frac{1}{\Gamma c_\alpha}\Lambda_{\alpha\gamma} \tag{3.6}$$

when a force is exerted on particle species γ. We will take Γ as the time unit in the representation of the Onsager coefficients; thus $\Gamma = 1$ in Eq. (3.6).

The simulation of drift in lattice gases when a force in one direction is imposed on the particles was pioneered in Ref. 6. The random-alloy model with a force imposed on one particle species was studied by simulations in Ref. 7. In that work a quantity related to the Onsager coefficients was deduced at very small vacancy concentrations only; hence no direct comparison will be made.

In our simulations the mean displacement of the particles is monitored; see Ref. 8 for a general review of the simulation procedures in lattice gases. Since small vacancy concentrations are investigated ($c_V \leq 0.1$) it is advantageous to attempt to move the vacancies in each single step. In fact, only the exchanges of A-V or B-V pairs are relevant. The time unit in the simulations is the Monte Carlo step per particle (MCS/p); within a Monte Carlo step each particle has *attempted* once, on the average, to make a transition to a neighbor site. Necessary redefinitions to keep transition probabilities in each direction ≤ 1 are included in the definition of the MCS/p.

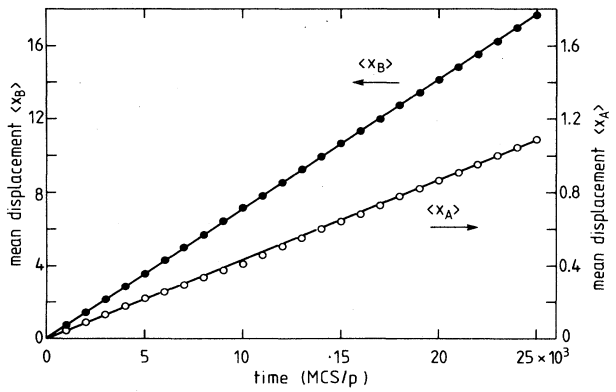

FIG. 1. Mean displacements of A (open circles) and B (solid circles) particles as a function of Monte Carlo steps. The concentrations were $c_A = c_B = 0.48$, the bias parameter $b = 1.1$, and the ratio of the transition rates $\Gamma_A/\Gamma_B = 0.1$. The number of sites was 50^3.

These details are irrelevant for the determination of the Onsager coefficients in the linear regime, but some care is appropriate to evaluate correctly the single-particle velocities used in Eq. (3.6). Since these details are rather technical, they are omitted here. Usually the B particles were taken as the faster species.

Figure 1 shows typical displacements of A and B particles where a force acts on the B particles and the A particles have a transition rate $\Gamma_A = \Gamma_B/10$. Note the different scales for the displacements of both species. It is seen that the drift of the A particles is reduced by a larger factor than 10. Namely, the A particles acquire their drift velocity indirectly through the collisions with the B particles. It can be shown for independent particles that the mean displacement is *self-averaging*, contrary to the mean-square displacement. Hence it suffices to monitor the displacements on one sample for sufficiently long times.

In the simulations with drift we used 50^3 sites in $D = 3$ and 400^2 sites in $D = 2$ and periodic boundary conditions were imposed. We took four different values of the bias parameter and run all programs with bias in the $+x$ and $-x$ directions. The number of MCS/p was chosen such that the equivalent single-particle displacements were always larger than 600. The simulation results were evaluated according to Eq. (3.6) and the results on $\Lambda_{\alpha\beta}/c_\alpha$ plotted. An example is given in Fig. 2. Lines were drawn by hand through the data points and the values for $b = 1$ taken as estimates for $\Lambda_{\alpha\beta}/c_\alpha$. The results on the Onsager coefficients will be discussed in the next section; here the validity of the procedure used will be discussed. Of course, the trivial test with a one-component lattice gas was made, where the Onsager coefficient is exactly $c(1-c)\Gamma$. A nontrivial test is provided by the lattice gas consisting of two species of particles with identical transition rates (to be visualized as identical but differently

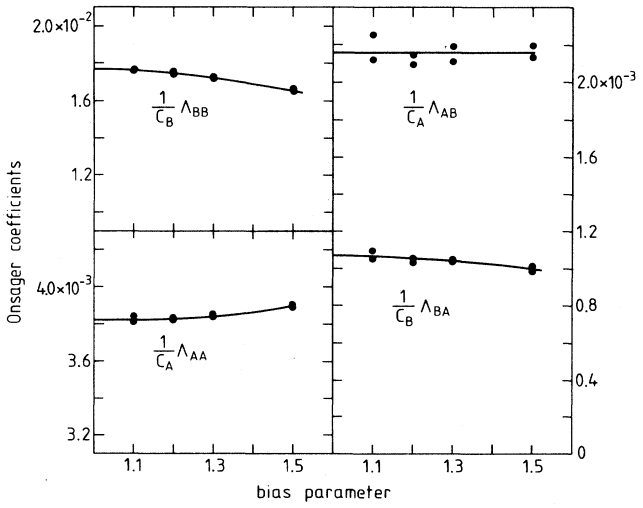

FIG. 2. Determination of Onsager coefficients $\Lambda_{\alpha\beta}/c_\alpha$ by extrapolation to bias parameter $b = 1$. The concentrations were $c_A = 0.64$, $c_B = 0.32$, and the ratio of the transition rates $\Gamma_A/\Gamma_B = 0.1$. The number of sites was 50^3.

colored particles). The Onsager coefficients of this two-component system are given by[1] (see also Sec. V)

$$\Lambda_{AB}=\frac{c_A c_B}{c}(1-c)[1-f(c)]\Gamma\ ,$$
$$\Lambda_{AA}=c_A(1-c)\Gamma-\Lambda_{AB}\ , \tag{3.7}$$
$$\Lambda_{BB}=c_B(1-c)\Gamma-\Lambda_{AB}\ ,$$

where $c=c_A+c_B$ is the summary particle concentration and $f(c)$ the corresponding correlation factor for tracer diffusion. This factor may be determined by simulations (see, e.g., Ref. 8); a sufficiently accurate approximation is provided by the theory of Nakazato and Kitahara.[9] We checked the validity of our procedure by simulation of the lattice gas with differently colored particles at several concentrations in $D=3$ and one concentration in $D=2$. An example is given in Fig. 3. The discrepancies between theory and simulations were at most 2%. Another indication of the accuracy is given by the difference of the data points for drift in the $+x$ or $-x$ direction. A somewhat better accuracy can be achieved in $D=2$, due to the stronger weight ($\frac{1}{2}$ instead of $\frac{1}{3}$) of the direction with a bias. We believe that the Onsager coefficients so determined have an accuracy of 2–3 %. Further points which corroborate the accuracy of the determinations are the fulfillment of the Onsager symmetry relations (see Sec. III B) and the very good description of interdiffusion provided by these coefficients (see Sec. IV). Of course, the accuracy could be increased by the use of more computing time, but this did not seem reasonable to us.

Very recently, exact relations between the Onsager coefficients of the random-alloy model, i.e., with noninteracting particles, were derived[10] from the correlation functions of linear-response theory. These relations are, in our conventions,

$$\Lambda_{AA}/\Gamma_A+\Lambda_{AB}/\Gamma_B=c_A(1-c)\ , \tag{3.8a}$$

$$\Lambda_{AB}/\Gamma_A+\Lambda_{BB}/\Gamma_B=c_B(1-c)\ , \tag{3.8b}$$

with c the summary concentration. We checked the validity of these relations by our simulation results (see Sec. III B).

B. Results

The results for the Onsager coefficients in three-dimensional two-component lattice gases are given in Table I. The dependence on the ratio of the concentrations is as expected from simple considerations. Note the good fulfillment of the Onsager symmetry relation $\Lambda_{AB}=\Lambda_{BA}$. It is also evident for $c_A=c_B$ and $\Gamma_A=\Gamma_B/10$ that the Onsager coefficients are approximately proportional to c_V, as is the case for $\Gamma_A=\Gamma_B$, cf. Eq. (3.7). The Onsager coefficients given in Table I will be further used in the following section. Table I also contains a test of the relations (3.8) derived recently.[10] It is seen from the third and fourth lines of each block that these relations are fulfilled within the accuracy of the simulations.

The results for the two-dimensional two-component lattice gases are represented in Figs. 4–6. In $D=2$ all simulations were performed with $c_V=0.04$. The special

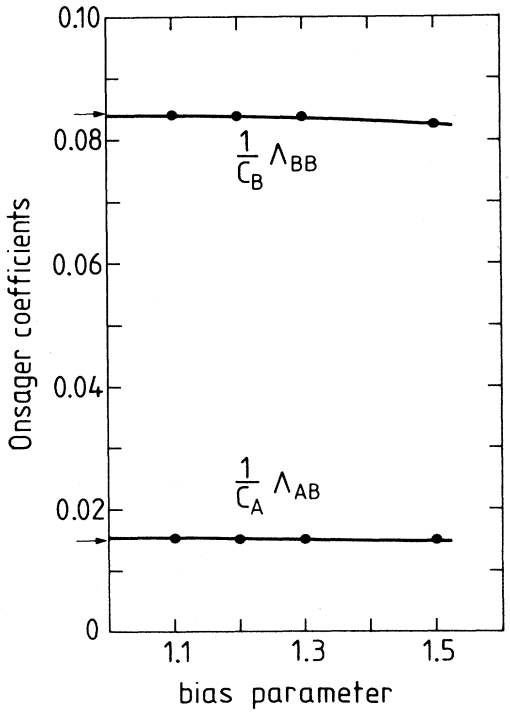

FIG. 3. Determination of Onsager coefficients $\Lambda_{\alpha\beta}/c_\alpha$ in the case of equal transition rates $\Gamma_A=\Gamma_B$ for $D=3$ dimensions and the concentrations $c_A=c_B=0.45$. The correlation factor at $c=0.9$ is $f(c)=0.697$ and the theoretical predictions according to (3.7) are indicated by arrows.

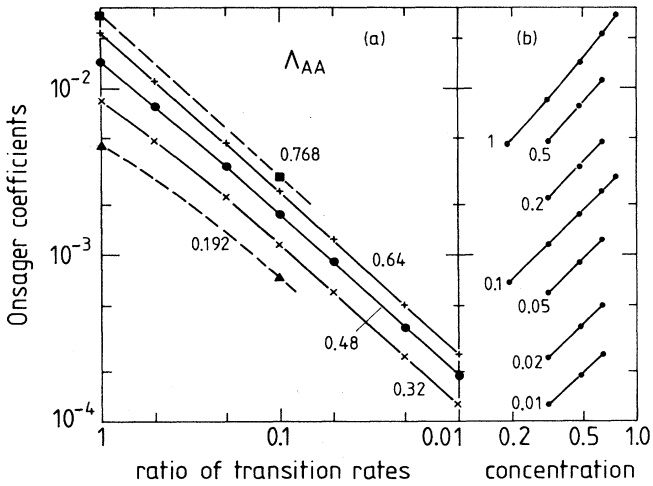

FIG. 4. Onsager coefficients Λ_{AA} of two-dimensional alloy systems. (a) Coefficients as functions of the ratio Γ_A/Γ_B of the transition rates; the concentration c_A is indicated as a parameter. (b) Coefficients as functions of c_A, with the ratio Γ_A/Γ_B as a parameter. All curves are guide lines to the eye.

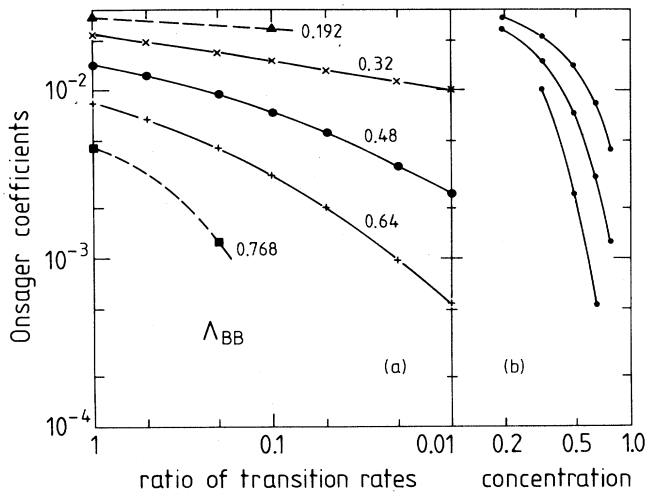

FIG. 5. Onsager coefficients Λ_{BB} of two-dimensional alloy systems. See Fig. 4 for more details.

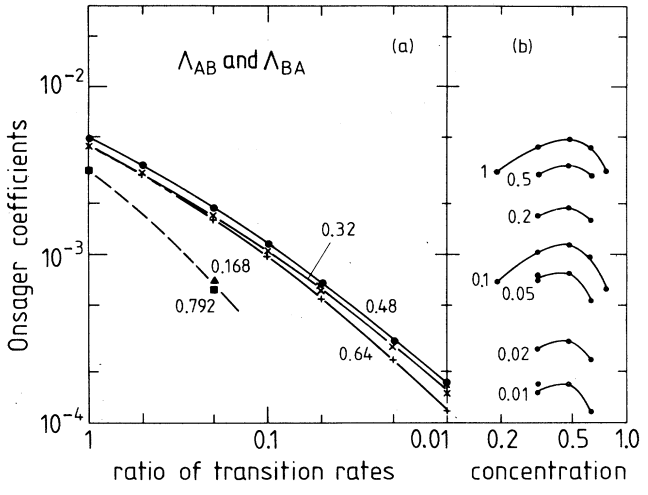

FIG. 6. Onsager coefficients Λ_{AB} and Λ_{BA} of two-dimensional alloy systems. See Fig. 4 for more details.

case $\Gamma_A=\Gamma_B$ is also included in the figures; it has been determined from Eq. (3.7) and verified for $c_A=0.48$. The following features emerge from the data.

(i) The Onsager coefficient Λ_{AA} is proportional to Γ_A/Γ_B, for large ratios of the transition rates. This coefficient describes the mobility of the slow species of particles in a background of rapidly moving particles. The limiting value for $\Gamma_A/\Gamma_B \ll 1$ is evidently

$$\Lambda_{AA}=c_A(1-c)\Gamma_A \ , \tag{3.9}$$

which is the appropriate generalization of the Onsager coefficient of the one-component system.

(ii) The Onsager coefficient Λ_{BB} seems to become proportional to Γ_A/Γ_B only for large concentrations c_A and large ratios of the transition rates. In fact, there should be two distinct regimes, according to whether c_A is larger or less than $1-c_{pV}$, where c_{pV} is the percolation concentration of the vacancies ($c_{pV}=0.592\,75$ for the square lattice). When $c_A>1-c_{pV}$, proportionality with Γ_A/Γ_B means that the B particles can only move as allowed by the motions of the A particles. In this regime the long-range mobility of the B particles vanishes when the A particles become immobile. When $c_A<1-c_{pV}$ there should be a limiting mobility of the B particles even for immobile A particles. The approach to the limiting behavior is not yet clearly seen in our data for $\Gamma_B/\Gamma_A=100$. A separate investigation of this regime with fixed A particles is planned. Of course, the limiting concentration $c_A=1-c_{pV}$ would lead to interesting behavior related to the percolation problem. Single-particle diffusion in this regime was studied by several authors.[11] The multiparticle aspect of this problem has also been investigated.[12]

TABLE I. Onsager coefficients and test of the relations (3.8) for random alloys in $D=3$ dimensions. The arrangement of the coefficients and of the right- and left-hand sides of (3.8) is shown in the first block. The ratio $\gamma=\Gamma_A/\Gamma_B$ was always 0.1. Note that $\Gamma_B=\Gamma$ and $\Gamma=1$ in our representation of the Onsager coefficients.

c_V \ c_A/c_B	1/2		1/1		2/1	
0.01	Λ_{AA}	Λ_{AB}	4.63×10^{-4}	1.91×10^{-4}		
	Λ_{BA}	Λ_{BB}	1.93×10^{-4}	2.96×10^{-3}		
	$\Lambda_{AB}+\Lambda_{AA}/\gamma$	$\Lambda_{BB}+\Lambda_{BA}/\gamma$	4.82×10^{-3}	4.87×10^{-3}		
	$c_A(1-c)$	$c_B(1-c)$	4.95×10^{-3}			
0.04	1.20×10^{-3}	5.38×10^{-4}	1.81×10^{-3}	7.15×10^{-4}	2.44×10^{-3}	6.85×10^{-4}
	5.50×10^{-4}	1.96×10^{-2}	7.49×10^{-4}	1.18×10^{-2}	6.91×10^{-4}	5.66×10^{-3}
	1.26×10^{-2}	2.50×10^{-2}	1.88×10^{-2}	1.90×10^{-2}	2.51×10^{-2}	1.25×10^{-2}
	1.28×10^{-2}	2.56×10^{-2}	1.92×10^{-2}		2.56×10^{-2}	1.28×10^{-2}
0.10			4.32×10^{-2}	1.53×10^{-3}		
			1.49×10^{-3}	2.97×10^{-2}		
			4.47×10^{-2}	4.50×10^{-2}		
			4.5×10^{-2}			

(iii) The Onsager symmetry relations $\Lambda_{AB}=\Lambda_{BA}$ are fulfilled in $D=2$ within the accuracy of the simulations.

(iv) The behavior of the cross coefficients as a function of concentrations and transition rates is intermediate between that of the diagonal coefficients. This is evident in view of relations (3.8). We could also verify the validity of these relations by our estimates for the Onsager coefficients in $D=2$. The accuracy was always similar to, or better than, the one in $D=3$. Thus, in the random-alloy model at given concentrations, ratio of the transition rates, and lattice type, there is only one independent Onsager coefficient.[10]

IV. INTERDIFFUSION

A. Theory

The theory of interdiffusion in the lattice-gas model with two species of particles is very simple, once the Onsager coefficients are known. It consists of solving the diffusion equation (2.25) with appropriate initial conditions. The equation reads

$$\frac{\partial}{\partial t}c_\alpha=\sum_\beta D_{\alpha\beta}\nabla^2 c_\beta \tag{2.25'}$$

and the coefficients $D_{\alpha\beta}$ are given in (2.24). This equation is decoupled by a linear transformation

$$c_\alpha=\sum_i e_{i\alpha}g_i\ , \tag{4.1}$$

where the eigenvectors $e_{\alpha i}$ and the corresponding eigenvalues λ_i follow from

$$\sum_\beta D_{\alpha\beta}e_{\beta i}=\lambda_i e_{\alpha i}\ . \tag{4.2}$$

Explicitly,

$$\lambda_\pm=\tfrac{1}{2}(D_{AA}+D_{BB})\pm\tfrac{1}{2}[(D_{AA}-D_{BB})^2+4D_{AB}D_{BA}]^{1/2} \tag{4.3}$$

and

$$\begin{aligned}&\mathbf{e}_i=m_i(D_{AB},\lambda_i-D_{AA})\ ,\\ &m_i=[D_{AB}^2+(\lambda_i-D_{AA})^2]^{-1/2}\ .\end{aligned} \tag{4.4}$$

A vector notation with respect to the particle index has been adopted.

Since the matrix $D_{\alpha\beta}$ is not symmetric but diagonalizable, one needs also the left eigenvectors,

$$\sum_\alpha f_{\alpha i}D_{\alpha\beta}=\lambda_i f_{\beta i}\ . \tag{4.5}$$

One finds

$$\begin{aligned}&\mathbf{f}_i=n_i(D_{BA},\lambda_i-D_{AA})\ ,\\ &n_i=[D_{BA}^2+(\lambda_i-D_{AA})^2]^{-1/2}\ .\end{aligned} \tag{4.6}$$

The left and right eigenvectors fulfill

$$\sum_{i=+,-} f_{\alpha i}e_{\beta i}=\nu\delta_{\alpha\beta} \tag{4.7}$$

and

$$\sum_{\alpha=A,B} f_{\alpha i}e_{\alpha j}=\nu\delta_{ij}\ , \tag{4.8}$$

where ν is a normalization factor whose explicit form will not be reproduced here.

We assume that we have initially a density profile given by a constant term plus one Fourier component as deviation,

$$c_\alpha(\mathbf{r},0)=c_\alpha+\delta c_\alpha(0)\cos(\mathbf{k}\cdot\mathbf{r})\ , \tag{4.9}$$

where the wave vector $\mathbf{k}$ is related to the wavelength of the deviation by $|\mathbf{k}|=2\pi/\lambda$. The solution of the diffusion equation yields

$$c_\alpha(\mathbf{r},t)=c_\alpha+\delta c_\alpha(t)\cos(\mathbf{k}\cdot\mathbf{r})\ ,$$

where

$$\delta c_\alpha(t)=\frac{1}{\nu}\sum_i\sum_\beta e_{\alpha i}f_{\beta i}\,\delta c_\beta(0)\exp(-\lambda_i k^2 t)\ . \tag{4.10}$$

We thus find the decay of the Fourier component as a superposition of two exponential decay modes. The decay constants are given by the eigenvalues λ_+,λ_- of the diffusivity tensor times k^2; the relative weight of the decay modes is determined by the initial conditions and the eigenvectors $\mathbf{e},\mathbf{f}$.

Before we compare solutions (4.10) with simulations, we consider two simplifying cases.

1. *Case of small vacancy concentration*

Here we discuss the general case where the interactions between the particles and the vacancies are included. If the following inequalities hold *simultaneously,*

$$\left[\frac{1}{c_A}+\chi_{AA}+\chi_{VV}-2\chi_{AV}\right]c_V\ll 1\ , \tag{4.11a}$$

$$\left[\frac{1}{c_B}+\chi_{BB}+\chi_{VV}-2\chi_{BV}\right]c_V\ll 1\ , \tag{4.11b}$$

$$(\chi_{AB}+\chi_{VV}-\chi_{AV}-\chi_{BV})c_V\ll 1\ , \tag{4.11c}$$

the solution $\lambda_\pm$ [Eq. (4.3)] may be expanded in c_V, and only the two leading orders need to be kept. Inserting Eq. (2.24) into Eq. (4.3) we first find

$$\lambda\pm=\frac{1}{2c_V}\left\{\Lambda_{AA}+2\Lambda_{AB}+\Lambda_{BB}+c_V\left[\Lambda_{AA}\left[\frac{1}{c_A}+\chi_{AA}+\chi_{VV}-2\chi_{AV}\right]+2\Lambda_{AB}(\chi_{AB}+\chi_{VV}-\chi_{AV}-\chi_{BV})+\Lambda_{BB}\left[\frac{1}{c_B}+\chi_{BB}+\chi_{VV}-2\chi_{BV}\right]\right]\right\}$$
$$\pm\frac{1}{2c_V}\left\{\left[\Lambda_{AA}-\Lambda_{BB}+c_V\Lambda_{AA}\left[\frac{1}{c_A}+\chi_{AA}+\chi_{VV}-2\chi_{AV}\right]-c_V\Lambda_{BB}\left[\frac{1}{c_B}+\chi_{BB}+\chi_{VV}-2\chi_{BV}\right]\right]^2+4\Lambda_{AA}\Lambda_{BB}[1+c_V(\chi_{AB}+\chi_{VV}-\chi_{AV}-\chi_{BV})]^2\right.$$
$$+4\Lambda_{AB}^2\left[1+c_V\left[\frac{1}{c_A}+\chi_{AA}+\chi_{VV}-2\chi_{AV}\right]\right]\left[1+c_V\left[\frac{1}{c_B}+\chi_{BB}+\chi_{VV}-2\chi_{BV}\right]\right]$$
$$+4\Lambda_{AB}\Lambda_{BB}[1+c_V(\chi_{AB}+\chi_{VV}-\chi_{AV}-\chi_{BV})]\left[1+c_V\left[\frac{1}{c_B}+\chi_{BB}+\chi_{VV}-2\chi_{BV}\right]\right]$$
$$\left.+4\Lambda_{AA}\Lambda_{AB}[1+c_V(\chi_{AB}+\chi_{VV}-\chi_{AV}-\chi_{BV})]\left[1+c_V\left[\frac{1}{c_A}+\chi_{AA}+\chi_{VV}-2\chi_{AV}\right]\right]\right\}^{1/2}. \quad (4.12)$$

Thus the square root in Eq. (4.12) can indeed be expanded linearly in c_V if Eqs. (4.11) hold, *irrespective of the values of the Onsager coefficients* Λ_{AA}, Λ_{AB}, and Λ_{BB}. This yields

$$\lambda_+\approx(\Lambda_{AA}+2\Lambda_{AB}+\Lambda_{BB})/c_V\ , \quad (4.13)$$

$$\lambda_-\approx\frac{\Lambda_{AA}\Lambda_{BB}-\Lambda_{AB}^2}{\Lambda_{AA}+2\Lambda_{AB}+\Lambda_{BB}}\left[\frac{1}{c_A}+\frac{1}{c_B}+\chi_{AA}+\chi_{BB}-2\chi_{AB}\right]. \quad (4.14)$$

From this result we recognize that in the considered limit $c_V\to 0$, Eq. (4.13) describes a fast mode, while Eq. (4.14) describes a slow mode. Since in this limit the Onsager coefficients Λ_{AA}, Λ_{AB}, Λ_{BB} themselves are proportional to c_V, the rate λ_+ tends to a finite nonzero limit for $c_V\to 0$, while λ_- becomes of the order of c_V. We shall show later that in this limit λ_+ describes the "density" relaxation (i.e., the relaxation of the total concentration c_A+c_B of both A and B particles) in the system, while λ_- describes interdiffusion. The diffusion coefficient for interdiffusion now has the familiar form of the product of a "kinetic factor" $(\Lambda_{AA}\Lambda_{BB}-\Lambda_{AB}^2)/(\Lambda_{AA}+2\Lambda_{AB}+\Lambda_{BB})$ and a "thermodynamic factor" $(c_A^{-1}+c_B^{-1}+\chi_{AA}+\chi_{BB}-2\chi_{AB})$. This thermodynamic factor can simply be interpreted as $[\partial^2(f/k_BT)/\partial c_A^2]_T$, using Eq. (2.3) with $c_V=0$ and noting that then $c_B=1-c_A$. [Remember that in Sec. II B we have relabeled the ϕ's as c's in order to distinguish global from locally varying quantities; actually in Eqs. (2.24) and (4.11)–(4.14) the c's can again be replaced by the ϕ's.] In this limit, it is also obvious that interactions χ_{AV}, χ_{BV}, χ_{VV} must cancel out from the results for λ_+,λ_-, as is evident from Eqs. (4.13) and (4.14), and that the interactions χ_{AA}, χ_{BB}, χ_{AB} do not enter separately but only in the familiar combination $\chi_{\rm eff}=\chi_{AA}+\chi_{BB}-2\chi_{AB}$. The result, Eq. (4.13), explicitly displays the "critical slowing down" of λ_- if we choose the parameters (temperature, concentration) such that we approach the "spinodal curve" of the mixture, where the large parentheses in Eq. (4.14) vanish. This is, of course, a typical mean-field result, and not to be expected to be valid beyond mean-field theory. However, since the present paper focuses attention on the noninteracting case, $\chi_{AA}=\chi_{BB}=\chi_{AB}=0$, the description of the "thermodynamic factor" in Eq. (4.14) is in fact then exact, since then the free energy only contains the expressions describing entropy of mixing. The latter are correctly given by Eq. (2.3).

We now wish to show that the two rates λ_+,λ_- in fact describe density relaxation and interdiffusion, in the considered limit. This is most simply seen if we specialize the general solution of the diffusion equation, Eq. (4.10), which is a superposition of two parts decaying with λ_+ and λ_-, to the special case where the initial condition in Eq. (4.9) has been such that the coefficient of either the term $\exp(-\lambda_+k^2t)$ or of the term $\exp(-\lambda_-k^2t)$ vanishes in Eq. (4.10). We can find the corresponding initial condition most simply by using the ansatz

$$c_A(\mathbf{r},t)=c_A+\delta c_A(0)\cos(\mathbf{k}\cdot\mathbf{r})\exp(-\lambda k^2t)\ , \quad (4.15a)$$

$$c_B(\mathbf{r},t)=c_B+\delta c_B(0)\cos(\mathbf{k}\cdot\mathbf{r})\exp(-\lambda k^2t) \quad (4.15b)$$

directly in the diffusion equation, Eq. (2.25), to find

$$\delta c_A(0)\left[-\lambda+\Lambda_{AA}\left[\frac{1}{c_A}+\frac{1}{c_V}+\chi_{AA}+\chi_{VV}-2\chi_{AV}\right]+\Lambda_{AB}\left[\frac{1}{c_V}+\chi_{AB}+\chi_{VV}-\chi_{AV}-\chi_{BV}\right]\right]$$
$$=-\delta c_B(0)\left[\Lambda_{AA}\left[\frac{1}{c_V}+\chi_{AB}+\chi_{VV}-\chi_{AV}-\chi_{BV}\right]+\Lambda_{AB}\left[\frac{1}{c_B}+\frac{1}{c_V}+\chi_{BB}+\chi_{VV}-2\chi_{BV}\right]\right]. \quad (4.16)$$

Here we have used the equation for $\partial c_A(\mathbf{r},t)/\partial t$; the equation $\partial c_B(\mathbf{r},t)/\partial t$ does not yield anything new, of course, if λ in Eqs. (4.15) and (4.16) is an eigenvalue. From Eq. (4.16) we hence find, in the limit where $c_V \to 0$,

$$\frac{\delta c_B(0)}{\delta c_A(0)} = -\frac{\Lambda_{AA}+\Lambda_{AB}-c_V\lambda}{\Lambda_{AA}+\Lambda_{AB}} . \tag{4.17}$$

If we consider the solution $\lambda=\lambda_-$, Eq. (4.14) shows that the term $c_V\lambda_-$ is of order c_V^2 and thus by a factor c_V smaller than the term $\Lambda_{AA}+\Lambda_{AB}$, which is of order c_V. Thus we conclude that the initial condition characterized by the ratio R_- of concentration amplitudes

$$R_- \equiv \delta c_B^-(0)/\delta c_A^-(0) = -1+O(c_V) \tag{4.18}$$

relaxes with λ_- only. But this is exactly the case of interdiffusion: for A and B particles, the initial concentration deviations from equilibrium are opposite in sign but equal in magnitude. In contrast, if we choose $\lambda=\lambda_+$ in Eq. (4.17), we obtain instead a ratio R_+ of concentration amplitudes, using Eq. (4.13)

$$R_+ \equiv \delta c_B^+(0)/\delta c_A^+(0) = (\Lambda_{AB}+\Lambda_{BB})/(\Lambda_{AB}+\Lambda_{AA}) > 0 . \tag{4.19}$$

Thus choosing $\delta c_A^+(0)$ and $\delta c_B^+(0)$ of the same sign, so that there is a variation of the "density" $c_A(\mathbf{r})+c_B(\mathbf{r})$, one obtains a mode relaxing only with λ_+. This relaxation, of course, is balanced by vacancies, and in the limit $c_V \to 0$ the weight of this density-relaxation mode turns to zero, for initial conditions which satisfy $\delta c_B(0) = -\delta c_A(0)$ which are then still possible.

One can turn this argument around and consider an initial condition $\delta c_B(0) = -\delta c_A(0)$ for the case of nonzero but small vacancy concentration. Then one finds that this initial condition decays with the two exponentials $\exp(-\lambda_+ k^2 t)$ and $\exp(-\lambda_- k^2 t)$, but the factor in front of $\exp(-\lambda_- k^2 t)$ stays of order unity for $\phi_V \to 0$ while the factor in front of the $\exp(-\lambda_+ k^2 t)$ term is of order ϕ_V.

We now discuss various limits of the "kinetic factor"

$$\Lambda_{\text{int}} \equiv (\Lambda_{AA}\Lambda_{BB}-\Lambda_{AB}^2)/(\Lambda_{AA}+2\Lambda_{AB}+\Lambda_{BB}) \tag{4.20}$$

in Eq. (4.14). If there are no crossterms, $\Lambda_{AB} \to 0$, it can be simply rewritten as $\Lambda_{\text{int}}^{-1} = \Lambda_{AA}^{-1} + \Lambda_{BB}^{-1}$, i.e., the reciprocals of the Onsager coefficients $\Lambda_{AA}, \Lambda_{BB}$ are additive to determine the reciprocal Onsager coefficient for interdiffusion. It is also interesting to consider the case where one species, say B, is much faster than the other species, i.e., $\Lambda_{BB} \gg \Lambda_{AA}, \Lambda_{AB}$. Then we find

$$\Lambda_{\text{int}} \approx \Lambda_{AA}(1-\Lambda_{AB}^2/\Lambda_{AA}\Lambda_{BB}) \times (1-2\Lambda_{AB}/\Lambda_{BB}-\Lambda_{AA}/\Lambda_{BB}) \approx \Lambda_{AA} , \tag{4.21}$$

if also $\Lambda_{AB}^2 \ll \Lambda_{AA}\Lambda_{BB}$: then interdiffusion is *solely determined by the Onsager coefficient Λ_{AA} of the slow component.* The physical interpretation of this result is very simple, of course: since there are so few vacancies present, the relaxation of the concentration deviation of the fast component is effectively blocked by the slow component, and only if a slow atom vacates a site can a fast one occupy it.

2. *Case of differently colored identical particles*

In the case $\Gamma_A = \Gamma_B = \Gamma$ we restrict the discussion to the noninteracting case, where the explicit expressions (3.7) for the Onsager coefficients are available. Very simple results are obtained for the eigenvalues from these expressions,

$$\lambda_+ = \Gamma , \qquad \lambda_- = (1-c)f(c)\Gamma . \tag{4.22}$$

The first eigenvalue is identical to the coefficient of collective diffusion in a one-component lattice gas.[13] The second eigenvalue represents the interdiffusion of the differently colored particles. By a similar derivation as the one leading to (4.17) and by use of (3.7) one finds that the relaxation of density variations is governed by λ_- only, for the following ratio of the amplitudes:

$$R_- \equiv \delta c_B^-(0)/\delta c_A^-(0) = -1 . \tag{4.23}$$

As expected, only slow relaxation occurs when there is no total concentration amplitude present. The larger eigenvalue λ_+ appears as a single relaxation mode only for the ratio

$$R_+ \equiv \delta c_B^+(0)/\delta c_A^+(0) = c_B/c_A . \tag{4.24}$$

For general ratios of the initial amplitudes, collective diffusion and interdiffusion take place concurrently. Equation (4.22) shows that the coefficient of interdiffusion is given, for $\Gamma_A = \Gamma_B$, by the coefficient of tracer diffusion at the summary concentration c. We will return to this result in the next section.

B. Simulation and results

The simulations were all done for the random-alloy model where, apart from the exclusion of double occupancy, no interactions of the particles and/or vacancies are considered. To simulate the interdiffusion of the two species, three- and two-dimensional lattices were occupied with A and B particles with cosinelike density profiles according to (4.9). The three-dimensional lattices normally had 80^3 sites; the case with $c_V = 0.01$ was investigated in samples with 120^3 sites. The two-dimensional lattices had 1000^2 sites. The occupation with particles was done in the following way: A wave vector $\mathbf{k}$ was chosen in the x direction with the wavelength λ in the range between 80 and $13\frac{1}{3}$ lattice constants. Also values of c_A, c_B, and $\delta c_A(0) = -\delta c_B(0)$ were selected. The initial concentrations of the lattice planes ($D=3$ dimensions) or rows ($D=2$ dimensions) perpendicular to the x direction were calculated from (4.9) and the sites were occupied with A or B particles with the corresponding probabilities. This method corresponds to given chemical potentials for the planes or rows. Hence there are fluctuations of the concentrations from their nominal values which are unimportant for the lattice sizes used. After the occupation step, the initial amplitudes were determined by fitting the expression (4.9) to the actual occupation numbers of the lattice planes or rows perpendicular to the x direction, using a standard fit routine. The

particles then performed the usual hopping processes in a lattice gas,[8] with transition rates Γ_A for the A and Γ_B for the B particles to vacant sites. Actually, transitions of the B particles were always executed when allowed by the presence of a vacancy, and the transition probabilities of the A particles were reduced according to the given ratio Γ_A/Γ_B. In regular time intervals the occupancies in the planes or rows perpendicular to the x direction were determined and the amplitudes $\delta c_\alpha(t)$ obtained by the fit routine. The interdiffusion was investigated for all concentrations and all ratios of the transition rates for which Onsager coefficients were estimated in $D=3$ and $D=2$ dimensions. Of course, we can only present a small selection of all data produced.

In the figures a comparison is made between the theory of Sec. IV A where the Onsager coefficients of Sec. III are used for the explicit evaluation of (4.10), and the simulation data. Figure 7 shows results in $D=3$ at $c_A=c_B=0.48$ and $\Gamma_A=\Gamma_B/10$, at three different wavelengths. There is very good agreement between the simulations and the theory curves, except at the shortest wavelength. In fact, whenever the amplitudes δc_α become less than about 10^{-2}, they show strong statistical scatter and hence are no longer reliable.

It is evident that two decay modes are present, especially in the decay of the density profile of the faster particles. To illustrate this point in more detail we show in Fig. 8 a simulation at a larger vacancy concentration ($c_V=0.1$) and in Fig. 9 at a small vacancy concentration ($c_V=0.01$). At the larger vacancy concentration, the rapid decay mode is clearly seen in the initial decay of the concentration profile of the B particles. Note that the concentration profile of the A particles decays initially

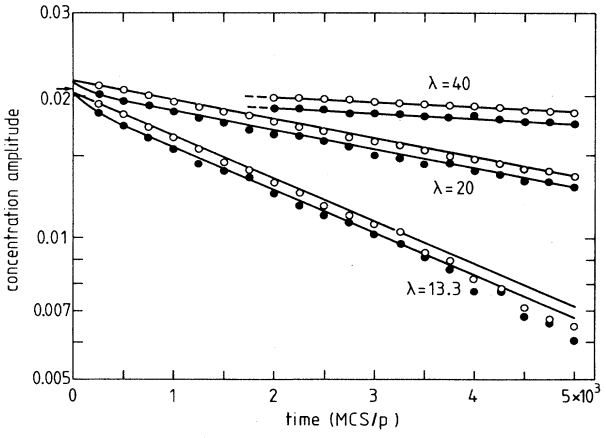

FIG. 7. Amplitudes of concentration profiles as a function of Monte Carlo steps per particle. The open circles (A particles) and the solid circles (B particles) are simulation data and the curves represent the theory of Sec. VI. The lattice had 80^3 sites, and three different wavelengths λ of the density variation are shown. The arrow indicates the initial concentration amplitudes for $\lambda=40$. The concentrations were $c_A=c_B=0.48$ and $\Gamma_A/\Gamma_B=0.1$.

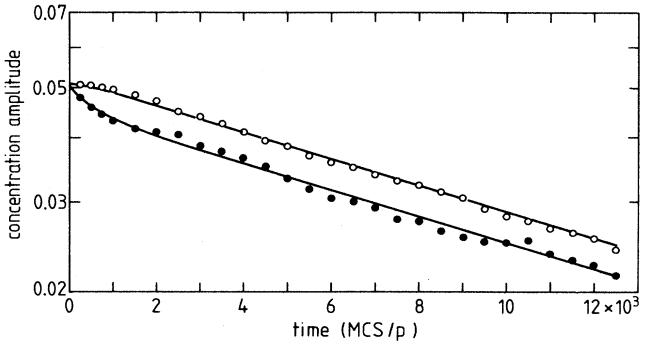

FIG. 8. Amplitudes of concentration profiles as a function of Monte Carlo steps per particle. Open circles, A particles; solid circles, B particles; lines, theory. The concentrations were $c_A=c_B=0.45$ and $\Gamma_A/\Gamma_B=0.1$. The wavelength was $\lambda=40$.

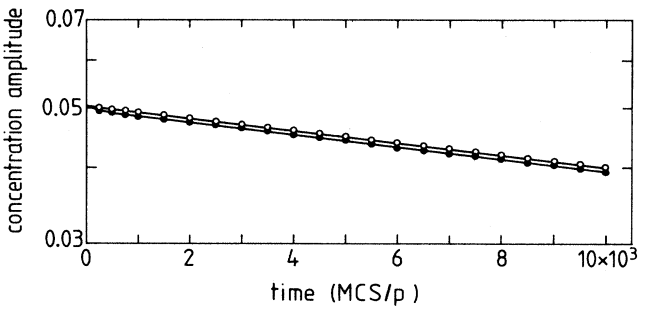

FIG. 9. Amplitudes of concentration profiles as a function of Monte Carlo steps per particle. Open circles, A particles; solid circles, B particles; lines, theory. The concentrations were $c_A=c_B=0.495$ and $\Gamma_A/\Gamma_B=0.1$. The wavelength was $\lambda=20$.

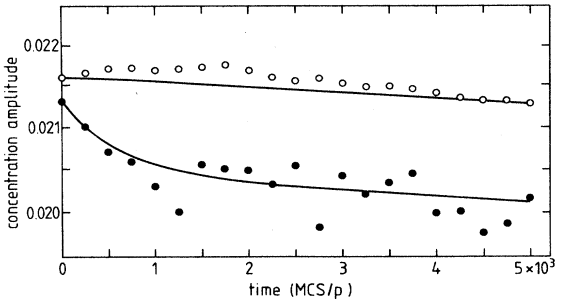

FIG. 10. Amplitudes of concentration profiles as a function of Monte Carlo steps per particle. Open circles, A particles; solid circles, B particles; lines, theory. The concentrations were $c_A=0.32$, $c_B=0.64$, and $\Gamma_A/\Gamma_B=0.01$. The number of lattice sites was 1000^2 and the wavelength $\lambda=33\frac{1}{3}$.

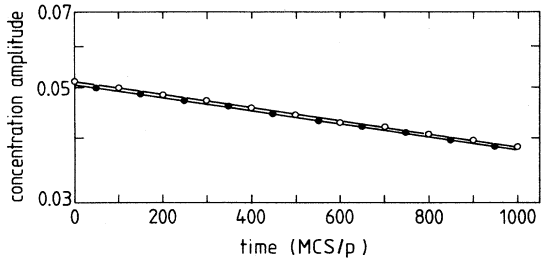

FIG. 11. Amplitudes of concentration profiles as a function of Monte Carlo steps per particle for the case $\Gamma_A=\Gamma_B$. Open circles, A particles; solid circles, B particles; given at alternating time points for clarity. The straight lines represent the theory as described in the text. The concentrations were $c_A=c_B=0.45$, and 12 samples were averaged.

even slower than at later times. The long-time decay of both concentration profiles is governed by the eigenvalue λ_-. We observe again very satisfactory agreement between the simulation results and the predictions of the theory. While at the vacancy concentration $c_V=0.1$, the initial amplitudes of the density profiles were smaller than the vacancy concentration; in the case $c_V=0.01$ they were 5 times as large as the corresponding vacancy concentration. In this case the fast decay mode is hardly noticeable in the figure. Evidently the small vacancy concentration allows only a partial relaxation of the concentration profile of the B particles; most of the relaxation of the profile occurs on the time scale of the slower mode, which determines also the decay of the A profile. The point is that this behavior is fully contained in the appropriate solution (4.10) of the diffusion equation. The eigenvalues *and* the initial conditions appear to describe completely the detailed behavior of the interdiffusion process. Figure 9 shows better agreement between theory and simulations and less fluctuations than the previous examples; this is due to the averaging over four samples.

To give an example for quite different parameters, and also for a simulation in $D=2$, we select the case $c_A=0.32$, $c_B=0.64$, and $\Gamma_A=\Gamma_B/100$. Figures 4 and 6 indicate that the Onsager coefficients Λ_{AA} and Λ_{AB} are very small in this case, resulting in a very small eigenvalue λ_-. We show in Fig. 10 the simulation results together with the theoretical prediction on a strongly expanded scale. On this scale the fluctuations of the data points are considerable. Nevertheless, we feel that the theory gives a very satisfactory description of the behavior of the interdiffusion observed in the simulations.

We finally consider the case of identical transition rates of both species of particles, $\Gamma_A=\Gamma_B$. As described in Sec. IV A, theory predicts a single exponential decay mode in this case when $\nabla c_A=-\nabla c_B$. The decay constant is proportional to the interdiffusion coefficient which is identical to the tracer-diffusion coefficient at the summary particle concentration $c=c_A+c_B$, cf. Eq. (4.22). We investigated by simulations interdiffusion of *two differently colored particles* at several ratios of c_A/c_B at $c_V=0.1$, and at $c_A=c_B$ for several vacancy concentrations. Figure 11 demonstrates that there is indeed only a single decay mode present in the simulation results. The solid lines represent exponential decay with $\exp(-\lambda_- k^2 t)$, and expression (4.22) for λ_-, corresponding to the tracer-diffusion coefficient, was calculated from the formula of Ref. 9. Since an average over 12 samples was performed, the scatter of the data points is small. We examined the independence of the decay constant on c_A/c_B by performing simulations at different ratios and

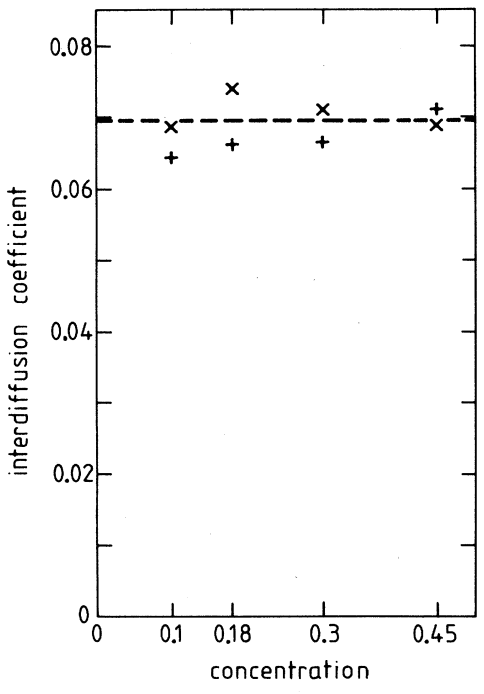

FIG. 12. Interdiffusion coefficient for two differently colored particles at different concentrations of one species. The lattice had 80^3 sites and $c_V=0.1$. Crosses, simulation data for $\lambda=80$; pluses, simulation data for $\lambda=40$; dashed line, theory.

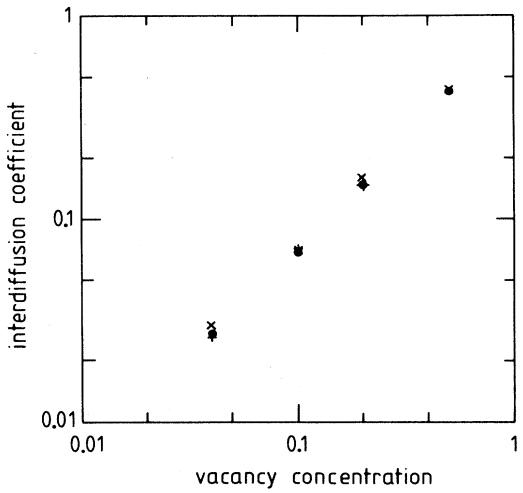

FIG. 13. Interdiffusion coefficient for two differently colored particles for different vacancy concentrations. Crosses, data for $\lambda=80$; pluses, data for $\lambda=40$; points, theory.

fitting the results to a single exponential decay. The resulting interdiffusion coefficients are given in Fig. 12, together with the theoretical prediction. The scatter of data is larger at $c_A \neq c_B$ since averages over only four samples were performed. The test of the dependence on the vacancy concentration c_V is given in Fig. 13. The deviations of the theory from the simulations appear to be small in this log-log plot; nevertheless, the agreement between theory and simulations is quite satisfactory.

C. Remarks

The following features of the interdiffusion of two species of particles in the random-alloy model with conserved particle and vacancy numbers emerge from theory and are corroborated by the simulations.

(i) The interdiffusion is characterized by the Onsager coefficients and the particle and vacancy concentrations. Once the Onsager coefficients are known, and the initial conditions specified, a quantitative prediction of the time development of the interdiffusion profile can be made.

(ii) From the diffusion equation follow two diffusion modes. There is a clear separation into a fast and slow mode for large ratios of the transition rates of both species (unless the faster species is not effectively blocked by absence of percolation conditions). The contributions of both modes to the development of interdiffusion profiles are influenced by the initial conditions. When the vacancy concentration is small, the contribution of the fast mode is reduced. Physically this corresponds to the situation that the fast component cannot attain equilibrium before the slow component has relaxed.

(iii) The interdiffusion of differently colored particles is described by a single diffusive mode; the corresponding diffusion coefficient is given by the tracer-diffusion coefficient in the lattice gas with the summary concentration.

V. TRACER DIFFUSION

A. Theory

The diffusion of tagged particles in the random-alloy model was treated in Ref. 1 in the frame of Onsager's formulation (see also Refs. 2 and 3). Since the previous authors used the assumption of complete thermal equilibrium of vacancies ($\mu_V \equiv 0$) which we do not use, because it does not hold for the model investigated and its simulations, we will give a brief outline of the derivations within our formulation. The results will be identical, since also in our treatment of *tracer diffusion* the chemical potential of the vacancies is kept constant, $\nabla \mu_V = 0$. Generalizing the derivations of Sec. II we consider four components A, A^*, B, V, or A, B, B^*, V, respectively, where A^* or B^* represent the (small) fraction of tagged particles. We obtain the following set of equations as an extension of (2.21):

$$\mathbf{j}_\alpha = -\beta \sum_\beta \Lambda_{\alpha\beta} \nabla(\mu_\beta - \mu_V) , \tag{5.1}$$

where the Greek indices now designate the species A, A^* (or B^*), and B. There are six Onsager coefficients $\Lambda_{\alpha\beta}$ and the symmetry property $\Lambda_{\alpha\beta} = \Lambda_{\beta\alpha}$ holds. Tracer diffusion can be derived by imposing gradients in the concentrations c_A and c_{A^*} of the species A and A^* with the conditions

$$c_A + c_{A^*} = \text{const}, \quad c_B = \text{const} ; \tag{5.2a}$$

that is,

$$\nabla c_A = -\nabla c_{A^*}, \quad \nabla c_B = 0 . \tag{5.2b}$$

One considers either the current density $\mathbf{j}_A$ induced by ∇c_A or $\mathbf{j}_{A^*}$ induced by ∇c_{A^*} and finds

$$D_t^{A^*} = \frac{1}{c_{A^*}} \Lambda_{A^* A^*} - \frac{1}{c_A} \Lambda_{A A^*} , \tag{5.3a}$$

$$D_t^{A} = \frac{1}{c_A} \Lambda_{AA} - \frac{1}{c_{A^*}} \Lambda_{A A^*} . \tag{5.3b}$$

Both expressions are equal and represent the tracer-diffusion coefficient D_t^A, since $\mathbf{j}_A = -\mathbf{j}_{A^*}$. They are the generalization of the formally identical expressions for the tracer-diffusion coefficient of A^* particles in a lattice gas with A and A^* but without B particles.

The first form is more commonly referred to in the literature (see, e.g., Refs. 3 and 14), but the second form (5.3b) exhibits more clearly the different processes influencing the tracer diffusion. The coefficient Λ_{AA}/c_A is related to the mobility of the A (and A^*) particles; this coefficient was investigated in Sec. III for vanishing concentrations c_{A^*}. Note that it depends on c_B and Γ_B as well. In the special case $c_B = 0$ and for noninteracting lattice gases it is given by $(1 - c_A)\Gamma_A$, in the limit $c_{A^*} \to 0$. The second term contains the correlation effects inherent in tracer diffusion.[15] This is evident from the special case $c_B = 0$ where the second term is

$$(1 - c_A)[1 - f(c_A)]\Gamma_A$$

and $f(c_A)$ is the correlation factor for tracer diffusion. If tracer diffusion of B^* particles is considered, one has

$$D_t^B = \frac{1}{c_{B^*}} \Lambda_{B^* B^*} - \frac{1}{c_B} \Lambda_{B B^*} = \frac{1}{c_B} \Lambda_{BB} - \frac{1}{c_{B^*}} \Lambda_{B B^*} . \tag{5.4}$$

An interesting special case is tracer diffusion in the lattice gas with identical transition rates of both species. Since the particles have identical properties, one can also consider gradients of the particles that obey

$$c_B + c_{A^*} = \text{const}, \quad c_A = \text{const} . \tag{5.5}$$

The condition $\mathbf{j}_A = 0$ yields for this case

$$\frac{1}{c_{A^*}} \Lambda_{A A^*} = \frac{1}{c_B} \Lambda_{AB} . \tag{5.6}$$

If a force is exerted on the tagged (A^*) particles, the velocity induced in the A particles is the same as in the B particles. The velocity would also be the same in a lattice

gas consisting of only A and A^* particles with the summary concentration c. Designating the Onsager coefficients of this lattice gas with (0) we have

$$\frac{\Lambda_{AA^*}}{\Lambda^{(0)}_{AA^*}} = \frac{c_A}{c} . \tag{5.7}$$

On the other hand, $\Lambda^{(0)}_{AA^*} = (1-c)[1-f(c)]\Gamma_A$, as discussed above. Equations (5.3), (5.6), and (5.7) allow us to derive the expression for Λ_{AB} given in (3.7). The other two coefficients are found from the fact that the eigenvalue λ_+ of (4.3) must describe collective diffusion in this case, i.e., $\lambda_+ = \Gamma$, as discussed in Ref. 13. Relations (3.7) were first derived in Ref. 1 (see also Refs. 2 and 3).

There are attempts to derive the tracer-diffusion coefficients of the random-alloy model with different ratios of the transition rates and general concentrations from microscopic theory.[16,17] Here we are interested in the analysis of tracer-diffusion coefficients in terms of Onsager coefficients and in the relation of tracer diffusion to interdiffusion. Therefore we will abstain from comparing our results with the microscopic theories.

B. Simulations and results

It is now a standard procedure to estimate tracer-diffusion coefficients in lattice gases by Monte Carlo simulations.[8] In our simulations, lattices of size $(40)^3$ in $D=3$ dimensions and $(250)^2$ in $D=2$ dimensions were used. Typical mean-square displacements of tagged A and B particles as a function of time are shown in Fig. 14. Although the transition rates of both species differ by a factor of 10, the difference in the tracer-diffusion coefficients is roughly a factor 5. This is due to the difference in the backward correlations for both particle species. Since the mean-square displacement is *not self-averaging,* it makes no sense to follow if for long times. Instead, one should use samples as large as possible. To achieve this aim, one may also split the time of a sufficiently long simulation into intervals, determine the mean-square displacements within these intervals, and average over them. The problem is to make sure that the *asymptotic* mean-square displacement is obtained in this way. Figure 15 shows the dependence of the estimated tracer-diffusion coefficients of B particles on the time interval over which the mean-square displacements were determined. Each simulation was run over 20 time intervals. There is a much stronger dependence of the estimated tracer-diffusion coefficients on the length Δt of the time interval in $D=2$ dimensions than in $D=3$ dimensions. The reason for this dependence is the presence of a logarithmic correction in the mean-square displacements in lattice gases in $D=2$ dimensions, as found in the one-component case.[18] We fitted our estimates $D_{\rm est}(\Delta t)$ in $D=2$ dimensions by (cf. Fig. 15)

$$D_{\rm est}(\Delta t) = a + b\ln(\Delta t)/\Delta t + d/\Delta t , \tag{5.8}$$

as suggested by the theoretical work, and took the coefficient a as our final estimates of the tracer-diffusion coefficients. In $D=3$ dimensions the apparent variation with Δt is smaller; thus we took the estimates for the largest time interval (e.g., $\Delta t = 5000$ MCS for $c_V = 0.04$) as our final ones.

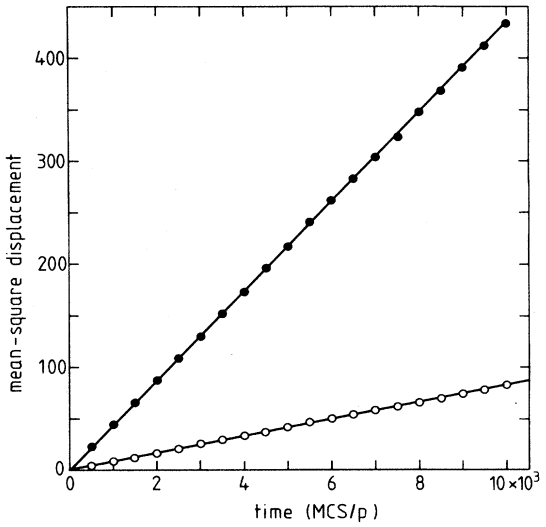

FIG. 14. Mean-square displacements of tagged A (open circles) and B (solid circles) particles as a function of Monte Carlo steps per particle. The lattice had 50^3 sites; the concentrations were $c_A = c_B = 0.45$ and $\Gamma_A/\Gamma_B = 0.1$.

Several groups[19–22] obtained previous results on tracer diffusion in random alloys in $D=3$ dimensions. Our results presented below deviate from the previous results where comparisons can be made, e.g., by about 15% from Ref. 20 at $c_V = 0.01$ and $\Gamma_A/\Gamma_B = 0.1$. In this work short effective time intervals *per particle* were taken. The agreement is better with Ref. 22 (about 4% at $c_V = 0.1$ and $\Gamma_A/\Gamma_B = 0.1$) where longer time intervals were used. The dependence of the estimates of tracer-diffusion coefficients on the time interval was carefully studied in $D=3$ dimensions for the single-component lattice gas.[23] We believe that our results for the random-alloy model are better than the previous ones in $D=3$ dimensions because of the long time intervals used and because our correlation factors are smaller than the published values.

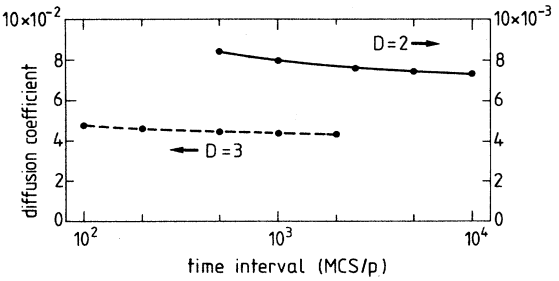

FIG. 15. Estimates of the tracer-diffusion coefficients as a function of the time intervals used. Data points are simulation results for B particles, and $\Gamma_A/\Gamma_B = 0.1$. $D=3$ dimensions: concentrations $c_A = c_B = 0.45$; the dashed line is a guide to the eye. $D=2$ dimensions: concentrations $c_A = c_B = 0.48$; the solid line represents the fit of the data by Eq. (5.8).

TABLE II. Tracer-diffusion coefficients and Onsager coefficients divided by concentrations for random alloys in $D=3$ dimensions. The ratio of the transition rates was $\Gamma_A/\Gamma_B=0.1$ and $\Gamma_B=\Gamma=1$. For each concentration the upper entry gives the coefficient for particle species A and the lower entry for species B.

c_A	c_V	D_t^α	$\Lambda_{\alpha\alpha}/c_\alpha$	$\Lambda_{\alpha\alpha^*}/c_{\alpha^*}$
0.495	0.01	7.77×10^{-4}	9.36×10^{-4}	1.6×10^{-4}
		3.46×10^{-3}	5.98×10^{-3}	2.5×10^{-3}
0.32	0.04	3.37×10^{-3}	3.76×10^{-3}	3.9×10^{-4}
		1.87×10^{-2}	3.07×10^{-2}	1.2×10^{-2}
0.48	0.04	3.18×10^{-3}	3.77×10^{-3}	5.9×10^{-4}
		1.51×10^{-2}	2.46×10^{-2}	9.5×10^{-3}
0.64	0.04	2.99×10^{-3}	3.82×10^{-3}	8.3×10^{-4}
		1.17×10^{-2}	1.77×10^{-2}	6.0×10^{-3}
0.45	0.1	8.31×10^{-3}	9.6×10^{-3}	1.3×10^{-3}
		4.36×10^{-2}	6.6×10^{-2}	2.2×10^{-2}

Table II gives our estimates for tracer-diffusion coefficients in $D=3$ dimensions and Table III for the ones in $D=2$ dimensions. The qualitative dependence on the relative concentrations c_A/c_B on the vacancy concentration in $D=3$ dimensions, and on the ratio of the transition rates in $D=2$ dimensions, is as expected from physical considerations. We have further analyzed the data by subtracting from the Onsager coefficients $\Lambda_{\alpha\alpha}/c_\alpha$ the tracer-diffusion coefficients. Equations (5.3) and (5.4) show that estimates for the Onsager coefficients $\Lambda_{\alpha\alpha^*}/c_{\alpha^*}$ are obtained in this way. Since two quantities with finite accuracy are subtracted, the errors of these numbers may be considerable, and are hard to estimate. Nevertheless, the dependencies on concentration and on the ratio of the transition rates are consistent and reasonable. Remember that these coefficients contain essentially the backward correlation of tagged-particle diffusion. For $\Gamma_A=\Gamma_B/100$ the reduction of the tracer-diffusion coefficient of A particles with increasing c_A is essentially

TABLE III. Tracer-diffusion coefficients and Onsager coefficients divided by concentrations for random alloys in $D=2$ dimensions. The vacancy concentration was $c_V=0.04$ and $\Gamma_B=\Gamma=1$. For each concentration the upper entry gives the coefficient for particle species A and the lower for species B.

c_A	Γ_A/Γ_B	D_t^α	$\Lambda_{\alpha\alpha}/c_\alpha$	$\Lambda_{\alpha\alpha^*}/c_{\alpha^*}$
0.192	1/10	3.08×10^{-3}	3.57×10^{-3}	4.9×10^{-4}
		1.29×10^{-2}	3.02×10^{-2}	1.73×10^{-2}
0.32	1/10	2.83×10^{-3}	3.59×10^{-3}	6.6×10^{-4}
		9.93×10^{-3}	2.34×10^{-2}	1.35×10^{-2}
0.48	1/10	2.57×10^{-3}	3.69×10^{-3}	1.08×10^{-3}
		7.21×10^{-3}	1.54×10^{-2}	8.2×10^{-3}
0.64	1/10	2.29×10^{-3}	3.76×10^{-3}	1.47×10^{-3}
		5.42×10^{-3}	9.70×10^{-3}	4.3×10^{-3}
0.768	1/10	2.10×10^{-3}	3.85×10^{-3}	1.75×10^{-3}
		4.44×10^{-3}	6.55×10^{-3}	2.1×10^{-3}
0.32	1/100	3.15×10^{-4}	3.95×10^{-4}	8.0×10^{-5}
		4.80×10^{-3}	1.60×10^{-2}	1.12×10^{-3}
0.48	1/100	2.77×10^{-4}	3.93×10^{-4}	1.16×10^{-4}
		1.83×10^{-3}	5.0×10^{-3}	3.2×10^{-3}
0.64	1/100	2.43×10^{-4}	3.94×10^{-4}	1.51×10^{-4}
		8.71×10^{-4}	1.68×10^{-3}	8.1×10^{-4}

due to this backward correlation, since Λ_{AA}/c_A is practically constant. The main point for the further discussion is that these coefficients are clearly present, although they are smaller than the diagonal coefficients.

C. Comparison with fast- and slow-mode theory

We now consider the relation of interdiffusion with tracer diffusion in the random-alloy model. In an atomistic model of a binary alloy, as well as in our computer simulation, there are only two kinetic rate factors, Γ_A and Γ_B, which describe the jumps of A or B particles to a vacant site, respectively. These rates then control both interdiffusion and self-diffusion of both species, for all concentrations of the alloy.

Thus the idea is fairly natural to assume that there must be a relation between the interdiffusion coefficient λ_- in Eq. (4.14) and the tracer-diffusion coefficients D_t^A, D_t^B. This would be very useful for the interpretation of experiments, where various methods exist to measure tracer-diffusion coefficients and then the interdiffusion coefficient could be predicted, while there are hardly any experimental possibilities to measure Onsager coefficients directly. Several approximations have been proposed in order to relate λ_- and D_t^A, D_t^B. Two of them have found a lot of recent attention in the literature on polymer mixtures and will be compared with the simulation results below. A deduction of the two proposals in the frame of our previous derivations will be given in the Appendix.

We examine whether there exists a relation of the slow eigenvalue λ_- to one of the following two averages.

(i) *Fast-mode theory*:

$$\langle D \rangle = (c_B D_t^A + c_A D_t^B)/c \ , \tag{5.9}$$

and (ii) *slow-mode theory*:

$$\langle D^{-1} \rangle^{-1} = c/(c_B/D_t^A + c_A/D_t^B) \ . \tag{5.10}$$

Of course, both expressions have to be compared with the eigenvalue λ_- which is characteristic of the long-time interdiffusion behavior. The eigenvalue λ_+ describes transient behavior, in particular collective diffusion in the case of two differently colored particles. For completeness it is also given in the following tables.

Table IV shows both averages, together with λ_+, λ_- for several random alloys in $D=3$ dimensions. It is obvious that neither the fast-mode theory nor the slow-mode theory applies. Although the differences between $\langle D^{-1} \rangle^{-1}$ and λ_- are of the order of 10% only, they are outside of the estimated error margins. Table V gives the same comparison for various random alloys in $D=2$ dimensions, for two different ratios Γ_A/Γ_B. Again, the slow-mode theory clearly does not apply for λ_-. In particular, for $\Gamma_A = \Gamma_B/100$ the differences are of the order of 20%. The agreement between fast-mode theory and λ_- at $c_A = 0.768$ and $\Gamma_A = \Gamma_B/10$ must be considered as fortuitous.

One particular point needs some discussion. The values for λ_- appear to be symmetric about $c_A = 0.5$ in $D=2$ dimensions, while they are slightly increasing with c_A in $D=3$ dimensions. We believe that this difference is real. In $D=2$ dimensions the samples with $c_A = 0.64$ are below the percolation threshold for motion of the B particles for fixed A particles; this results in a reduced mobility of the B component in the general case. In $D=3$ dimensions the sample with $c_A = 0.64$ is still above the percolation threshold and the mobility of B particles is correspondingly larger. We have examined that all Onsager coefficients used in deriving λ_+, λ_- at $c_A = 0.64$ give excellent fits of the corresponding interdiffusion data. Of course, further investigation is necessary to confirm this point in detail; however, this will not be done here.

In summary, neither the slow-mode nor the fast-mode theory can describe interdiffusion in the random-alloy model for $\Gamma_A \neq \Gamma_B$, in the long-time limit. A trivial exception is the case $\Gamma_A = \Gamma_B$ where the slow-mode and fast-mode theories coincide and where the coefficient of interdiffusion *is* given by the tracer-diffusion coefficient, at the summary concentration.

Also, attempts were made to relate the Onsager coefficients $\Lambda_{\alpha\beta}$, which characterize the transport properties of nontagged particles, to the tracer-diffusion coefficients. An early attempt is found in Ref. 24, and a refined connection was developed in Refs. 25–27. A transparent derivation of the approximate relations between $\Lambda_{\alpha\beta}$ and D_t^α of Refs. 25–27 was given in Ref. 28 (see also the review in Ref. 3). They are, in our notation,

$$\Lambda_{\alpha\beta} = c_\alpha D_t^\alpha \left[\delta_{\alpha\beta} + \frac{1-f(c)}{f(c)} \frac{c_\beta D_t^\beta}{\sum_\gamma c_\gamma D_t^\gamma} \right] . \tag{5.11}$$

A slight generalization to finite vacancy concentrations has been made and $f(c)$ is the correlation factor for tagged-particle diffusion in a lattice gas with summary concentration $c = c_A + c_B$. The relations are obviously valid for the case of identical transition rates [cf. (3.7)]. We examined these relations for $\Gamma_A \neq \Gamma_B$ by using our es-

TABLE IV. Comparison with fast-mode and slow-mode theories of interdiffusion for random alloys in $D=3$ dimensions. The ratio of the transition rates was always $\Gamma_A/\Gamma_B = 0.1$.

c_A	c_V	$\langle D \rangle$	$\langle D^{-1} \rangle^{-1}$	λ_+	λ_-
0.495	0.01	2.12×10^{-3}	1.27×10^{-3}	0.386	1.41×10^{-2}
0.32	0.04	8.48×10^{-3}	4.64×10^{-3}	0.577	4.92×10^{-3}
0.48	0.04	9.14×10^{-3}	5.25×10^{-3}	0.399	5.65×10^{-3}
0.64	0.04	8.80×10^{-3}	5.94×10^{-3}	0.251	6.49×10^{-3}
0.45	0.1	2.60×10^{-2}	1.40×10^{-2}	0.432	1.44×10^{-2}

TABLE V. Comparison with fast-mode and slow-mode theories of interdiffusion for random alloys in $D=2$ dimensions. The vacancy concentration was always $c_V=0.04$.

c_A	Γ_A/Γ_B	$\langle D\rangle$	$\langle D^{-1}\rangle^{-1}$	λ_+	λ_-
0.192	1/10	5.04×10^{-3}	3.63×10^{-3}	0.666	3.95×10^{-3}
0.32	1/10	5.20×10^{-3}	3.72×10^{-3}	0.478	4.13×10^{-3}
0.48	1/10	4.89×10^{-3}	3.79×10^{-3}	0.301	4.24×10^{-3}
0.64	1/10	4.38×10^{-3}	3.72×10^{-3}	0.195	4.12×10^{-3}
0.768	1/10	3.97×10^{-3}	3.63×10^{-3}	0.143	3.97×10^{-3}
0.32	1/100	1.81×10^{-3}	4.57×10^{-4}	0.282	5.45×10^{-4}
0.48	1/100	1.05×10^{-3}	4.81×10^{-4}	0.0781	5.90×10^{-4}
0.64	1/100	6.62×10^{-4}	4.68×10^{-4}	0.0271	5.50×10^{-4}

timates for the tracer-diffusion and Onsager coefficients. They are in variance with our numerical results, at all concentrations, in $D=2$ and 3 dimensions. For $\Gamma_A=\Gamma_B/10$ the typical differences are of the order of 10%. The case $\Gamma_A=\Gamma_B/100$ and $D=2$ dimensions is shown in Table VI. We point out that we have studied the case with conserved number of vacancies; the case with $\mu_V\equiv0$ requires a separate investigation. We conclude by noting that, generally, the tracer-diffusion coefficients contain additional Onsager coefficients, for instance, Λ_{AA^*}/c_{A^*}. These coefficients are characteristic of the backward correlations in the tagged-particle diffusion; they are not directly related to the Onsager coefficients entering the interdiffusion.

VI. DISCUSSION

We have studied the mobility, interdiffusion, and tracer diffusion in the random-alloy model with two different species of particles. In this model the particle numbers of both species and the numbers of vacancies are conserved. A grand-canonical ensemble with varying particle and vacancy numbers N_A, N_B, and N_V was introduced to derive the chemical potentials μ_A, μ_B, and μ_V. However, we did not make the assumption that the number of vacancies is regulated by the equilibrium condition $\mu_V\equiv0$.

For the formulation of transport theory we returned to the canonical ensemble and required locally the validity of the continuity equations, which are equivalent to global conservation of the numbers N_A, N_B, and N_V. The particle currents were related to the gradients of the chemical potentials by the Onsager coefficients. The local condition that the sum of the fractional occupancies of both particle species and of the vacancies is unity allowed us to eliminate the Onsager coefficients connected to the vacancies. There remain three Onsager coefficients for the alloy model with two particle species. They were estimated from numerical simulations of their mobilities when forces acted on one of the two species. The combination of the constitutive current relations with the continuity equations lead to coupled diffusion equations for both particle species. The solution of these equations exhibits two decay modes that are determined by the three Onsager coefficients. The weight of these decay modes is also influenced by the initial conditions. The slow decay mode describes the long-time behavior of interdiffusion.

The tracer diffusion, where the motion of tagged particles is monitored, contains additional off-diagonal Onsager coefficients. These coefficients contain the typical backward correlations of tagged-particle diffusion. Since these correlations have a different physical origin, one cannot expect that interdiffusion is simply related to tracer diffusion. Already from the form of the decay constants for interdiffusion one concludes that they cannot be expressed as averages, or inverse averages, of the tracer-diffusion coefficients. These statements are corroborated by the results of the numerical simulations. An exception is the case of identical transition rates of both particle species, where the coefficient of interdiffusion is given by the coefficient of tracer diffusion at the summary concentration of the lattice gas.

So far a consistent picture of mobility, interdiffusion, and tracer diffusion in the random-alloy model has been developed, which is supported by the numerical simulations. Why were different and sometimes conflicting conclusions reached in the field of metal and polymer physics?

The basic assumption of the treatment of interdiffusion in metal physics is the assumption of adjustment of the local vacancy concentration by the condition $\mu_V\equiv0$ (cf. Refs. 1–3 and 24–27). This requires the possibility for

TABLE VI. Comparison of Onsager coefficients according to (5.11) with the numerical estimates in $D=2$ dimensions, for $\Gamma_A=\Gamma_B/100$ and $c_V=0.04$. The value $f(0.96)=0.487$ was used, and the coefficients $\Lambda_{\alpha\beta}$ are arranged as matrices.

	c_A = 0.32		0.48		0.64	
Relation (5.11)	1.04×10^{-4}	1.03×10^{-4}	1.51×10^{-4}	1.22×10^{-4}	2.14×10^{-4}	1.05×10^{-4}
	$\equiv\Lambda_{AB}$	6.21×10^{-3}	$\equiv\Lambda_{AB}$	1.68×10^{-3}	$\equiv\Lambda_{AB}$	4.67×10^{-4}
Numerical	1.26×10^{-4}	1.49×10^{-4}	1.89×10^{-4}	1.70×10^{-4}	2.52×10^{-4}	1.18×10^{-4}
estimates	1.70×10^{-4}	1.02×10^{-2}	1.73×10^{-4}	2.40×10^{-3}	1.15×10^{-4}	5.38×10^{-4}

immediate creation and destruction of vacancies. In the thermodynamic formulation, vacancy creation and destruction is regulated by the introduction of a free enthalpy for vacancy formation, such that $\mu_V \equiv 0$ can be maintained at each instant and place. Physically, vacancies may be created and destroyed at lattice imperfections, in particular at dislocations. Instructive figures of the influence of these processes on transport properties are given, e.g., in Ref. 2. The resulting motion of whole lattice planes is called the Kirkendall effect, or also *bulk flow* of matter. It has been experimentally observed in metals, although its quantitative description requires the existence of efficient vacancy sinks; the fulfillment of the condition $\mu_V \equiv 0$ seems to be difficult in practice.[2]

There are flows of atoms in our lattice-gas models, and time-dependent shifts of the equivalent center of mass. For instance, the results of Fig. 8 imply first a flow of B particles into the A particles, followed by a slow counterflow of A particles and a reduced flow of the B particles. However, any marker associated with a lattice *plane* would not move. There is no bulk flow and no Kirkendall effect possible in our models, by their construction. It is not surprising that our results are different from analyses where different initial assumptions are made. Models with vacancy creation and destruction are difficult to implement in numerical simulations. One possibility is probably given by diffusion processes mediated by interstitial mechanisms. Other processes, such as creation and destruction of vacancies at dislocations, are certainly very difficult to model.

One particular aim of a coherent theoretical description of self-diffusion and interdiffusion in mixtures, which is often addressed in the literature,[1–5,15,24–36] is the idea to express the interdiffusion coefficient in terms of a "kinetic factor," involving self-diffusion coefficients of the diffusing species, and a "thermodynamic factor" which describes the thermodynamic driving force for interdiffusion. This question has found particular attention for fluid polymer mixtures recently, both theoretically[29–33,37] and experimentally[38–45] (see Ref. 4 for a short review). Empirically sometimes[38–41] the data seemed to be more consistent with the "slow-mode theory" (Refs. 31–33) and sometimes[42,43,45] with the "fast-mode theory" (Refs. 29 and 30). Now it would not be a surprise if, for fluid polymer mixtures, effects due to *bulk flow* are important, but a first-principles theory which includes such effects is rather difficult.[4,37] In the present model, bulk flow is strictly absent by construction, and naively one might think that then the slow-mode theory [Eq. (5.10)] should be applicable. However, our numerical results show that such a simple relation between tracer-diffusion coefficients and the interdiffusion coefficient does not exist, although the relation between interdiffusion and the Onsager coefficients works out nicely. Our results demonstrate clearly that *the hypothetical relations between tracer-diffusion coefficients and the Onsager coefficients* $\Lambda_{AA}, \Lambda_{BB}$ *in the mixture,* Eqs. (A4a) and (A4b), *do not hold, and also the neglect of the crossterm* Λ_{AB} *is not warranted.* Since these assumptions enter the alternative formula [Eq. (5.9)] as well, we are very skeptical whether any of these simple formulas describes a real system. From our point of view, it is no surprise that the comparison between experimental results and such oversimplified theoretical relations leads to ambiguous results, both for mixtures of small molecules[46] and for polymer mixtures.[4] We hope that the comparisons between computer simulations and the various theoretical approaches will shed light on the significance of similar comparisons between real experimentals and various theories, too.

ACKNOWLEDGMENTS

We thank E. J. Kramer, A. B. Lidiard, K. Schroeder, and H. Sillescu for stimulating discussions. The assistance of H. Jungbluth and K. Kutzbach with numerical work is also gratefully acknowledged.

APPENDIX: APPROXIMATIONS PROPOSED TO RELATE INTERDIFFUSION AND TRACER DIFFUSION IN THE LIMIT $c_V \to 0$

In this Appendix derivations of the so-called "slow-mode" and "fast-mode" theories are discussed. The former theory will be deduced from the results of Sec. IV A, while the latter theory is obtained by introducing the condition of complete thermal equilibrium.

1. The "slow-mode" theory

Suppose we apply Eq. (4.14) to a mixture where the B particles are nothing but tracer atoms A^*. Then we have

$$D_t^A = \lim_{c_{A^*} \to 0} \left[\frac{\Lambda_{AA}\Lambda_{A^*A^*} - \Lambda_{AA^*}^2}{\Lambda_{AA} + 2\Lambda_{AA^*} + \Lambda_{A^*A^*}} \left(\frac{1}{c_A} + \frac{1}{c_{A^*}} \right) \right] . \tag{A1}$$

Now D_t^A tends to a nonzero finite limit for zero tracer concentration. This is only possible if the kinetic factor in Eq. (A1) is also proportional to c_{A^*}. A plausible expression hence is [cf. also Eq. (3.7)]

$$\begin{aligned} \Lambda_{AA} &= \lambda_{AA} c_A , \\ \Lambda_{A^*A^*} &= \lambda_{A^*A^*} c_{A^*} , \\ \Lambda_{AA^*} &= c_A c_{A^*} \lambda_{AA^*} , \end{aligned} \tag{A2}$$

which yields

$$D_t^A = \lambda_{A^*A^*} = \lambda_{AA} , \tag{A3}$$

where in the last equality we have invoked the fact that there is no chemical distinction between A and A^*. Comparison of Eqs. (A2) and (5.3) then shows

$$\Lambda_{AA} = D_t^A c_A ; \tag{A4a}$$

a similar reasoning for an AB mixture where the A particles are tracer atoms B^* yields, of course,

$$\Lambda_{BB} = D_t^B c_B . \tag{A4b}$$

Note that Eq. (A4a) is true for a "mixture" without B particles, and Eq. (A4b) is true for a "mixture" without

A particles. Let us assume, however, that these relations remain valid if the other species of particles is added, and that the cross term Λ_{AB} in Eq. (4.14) can be neglected: With *these two assumptions,* which have no further physical justification to our knowledge, Eq. (4.14) becomes in the noninteracting case

$$\lambda_- = \frac{c_A c_B D_t^A D_t^B}{c_A D_t^A + c_B D_t^B} \left[\frac{1}{c_A} + \frac{1}{c_B} \right] , \tag{A5}$$

which is Eq. (5.10). It is called "slow-mode" theory because the slowly diffusing species clearly controls the interdiffusion coefficient.

2. The "fast-mode" theory

A rather different result, Eq. (5.9) can be obtained by several distinct arguments. We reproduce only one particular line of reasoning here. Let us return to Eq. (2.21) and arbitrarily assume that the interdiffusion proceeds such that everywhere the vacancy concentration $c_V(\mathbf{r},t)$ is in complete thermal equilibrium, i.e.,

$$\nabla \mu_V = \mathbf{0} . \tag{A6}$$

In view of Eq. (2.6c), Eq. (A6) cannot be justified. But the motivation for Eq. (A6) is that for real physical alloy there is no strict conservation of lattice sites, vacancies can be created and destroyed by interaction with other lattice imperfections (interstitials, dislocations, grain boundaries, external free surfaces, etc.), and then Eq. (A6) may be reasonable. If we now set, again neglecting crossterms,

$$\begin{aligned} \mathbf{j}_A &= -\beta \Lambda_{AA} \nabla \mu_A , \\ \mathbf{j}_B &= -\beta \Lambda_{BB} \nabla \mu_B , \\ \mathbf{j}_V &= -(\mathbf{j}_A + \mathbf{j}_B) . \end{aligned} \tag{A7}$$

The total flux $\mathbf{j}_A^T$ of A across a plane fixed with respect to the coordinate system is the sum of the diffusion flux of A plus A transported by the vacancy flux:

$$\mathbf{j}_A^T = -\beta \Lambda_{AA} \nabla \mu_A + c_A (\beta \Lambda_{AA} \nabla \mathbf{j}_A + \beta \Lambda_{BB} \nabla \mu_B) . \tag{A8}$$

Conservation of A particles implies

$$\frac{\partial c_A(\mathbf{r},t)}{\partial t} = \nabla(-\mathbf{j}_A^T) \tag{A9}$$

and using Eqs. (2.6a) and (2.6b) for $\phi_V \to 0$ one then obtains

$$\frac{\partial c_A(\mathbf{r},t)}{\partial t} = D_{\text{int}} \nabla^2 c_A(\mathbf{r},t) , \tag{A10}$$

where in the noninteracting case the interdiffusion coefficient becomes

$$D_{\text{int}} = \left[\frac{c_B}{c_A} \Lambda_{AA} + \frac{c_A}{c_B} \Lambda_{BB} \right] = c_B D_t^A + c_A D_t^B , \tag{A11}$$

invoking once more that Eqs. (A4a) and (A4b) can be used for the mixture as well. Since for $c_V \to 0$, $c_A + c_B = c = 1$, this is Eq. (5.9).

[1] E. Howard and A. B. Lidiard, Rep. Prog. Phys. **27**, 161 (1964).
[2] C. P. Flynn, *Point Defects and Diffusion* (Clarendon, Oxford, 1972).
[3] A. R. Allnatt and A. B. Lidiard, Rep. Prog. Phys. **50**, 373 (1987).
[4] K. Binder and H. Sillescu, in *Encyclopedia of Polymer Science and Engineering,* 2nd ed., edited by J. L. Kroschwitz (Wiley, New York, in press).
[5] J. W. Cahn and F. C. Larché, Scr. Metall. **17**, 927 (1983).
[6] G. E. Murch and R. J. Thorn, Philos. Mag. **36**, 529 (1977).
[7] G. E. Murch, Philos. Mag. A **46**, 151 (1982).
[8] K. W. Kehr and K. Binder, in *Applications of the Monte Carlo Method in Statistical Physics,* Vol. 36 of *Topics in Current Physics,* edited by K. Binder (Springer, New York, 1987), p. 181.
[9] K. Nakazato and K. Kitahara, Prog. Theor. Phys. **64**, 2261 (1980).
[10] L. K. Moleko and A. R. Allnatt, Philos. Mag. A **58**, 677 (1988).
[11] R. Kutner and K. W. Kehr, Philos. Mag. **48**, 199 (1983); R. B. Pandey and D. Stauffer, Phys. Rev. Lett. **51**, 527 (1983); J. Stat. Phys. **34**, 427 (1984).
[12] L. Heupel, J. Stat. Phys. **42**, 541 (1986).
[13] R. Kutner, Phys. Lett. **81A**, 239 (1981).
[14] G. E. Murch, Solid State Ionics **7**, 177 (1982).
[15] J. Bardeen and C. Herring, in *Imperfections in Nearly Perfect Crystals,* edited by W. Shockley (Wiley, New York, 1952), p. 261.
[16] R. A. Tahir-Kheli, Phys. Rev. B **28**, 2257 (1983); **28**, 3049 (1983).
[17] P. C. W. Holdsworth and R. J. Elliott, Philos. Mag. A **54**, 601 (1986).
[18] H. van Beijeren and R. Kutner, Phys. Rev. Lett. **55**, 238 (1985).
[19] H. J. de Bruin, G. E. Murch, H. Bakker, and L. P. van der Mey, Thin Solid Films **25**, 47 (1975).
[20] H. J. de Bruin, H. Bakker, and L. P. van der Mey, Phys. Status Solidi B **82**, 581 (1977).
[21] A. R. Allnatt and E. L. Allnatt, Philos. Mag. A **49**, 625 (1984).
[22] N. El-Meshad and R. A. Tahir-Kheli, Phys. Rev. B **32**, 6176 (1985).
[23] R. A. Tahir-Kheli, Phys. Rev. B **35**, 5503 (1987).
[24] L. S. Darken, Trans. AIME **175**, 184 (1948).
[25] J. R. Manning, Acta Metall. **15**, 817 (1967).
[26] J. R. Manning, *Diffusion Kinetics for Atoms in Crystals* (Van Nostrand, Princeton, 1968).
[27] J. R. Manning, Metall. Trans. **1**, 499 (1970).
[28] A. B. Lidiard, Acta Metall. **34**, 1487 (1986).
[29] E. J. Kramer, P. Green, and C. J. Palmstrom, Polym. **25**, 473 (1984).
[30] H. Sillescu, Makromol. Chem. Rapid Commun. **5**, 519 (1984); **8**, 393 (1987).
[31] F. Brochard, J. Jouffray, and P. Levison, Macromolecules **16**, 1638 (1983).
[32] K. Binder, J. Chem. Phys. **79**, 6387 (1983); Colloid Polym. Sci. **265**, 273 (1987).

[33]F. Brochard and P. G. de Gennes, Europhys. Lett. **1**, 221 (1985); A. Z. Akcasu, M. Benmouna, and H. Benoit, Polym. **27**, 1935 (1986).
[34]J. Crank, *The Mathematics of Diffusion,* 2nd ed. (Clarendon, Oxford, 1975).
[35]B. C. H. Stelle, in *Fast Ion Transport in Solids,* edited by W. van Gool (North-Holland, Amsterdam, 1973), p. 103.
[36]A. D. Le Claire, Philos. Mag. **3**, 921 (1958).
[37]W. Hess and A. Z. Akcasu (unpublished).
[38]U. Murschall, E. W. Fischer, Ch. Herkt-Maetzky, and G. Fytas, J. Polym. Sci., Polym. Lett. Ed. **24**, 191 (1986).
[39]G. Fytas, Macromolecules **20**, 1430 (1987); J. Kanetakis and G. Fytas, J. Chem. Phys. **87**, 5048 (1987).
[40]M. G. Brereton, E. W. Fischer, G. Fytas, and U. Murschall, J. Chem. Phys. **86**, 5174 (1987).
[41]J. S. Higgins, H. A. Fruitwala, and P. E. Tomlins (unpublished).
[42]D. A. Jones, J. Klein, and A. M. Donald, Nature (London) **321**, 161 (1986).
[43]R. J. Composto, E. J. Kramer, and D. M. White, Nature (London) **328**, 234 (1987).
[44]R. W. Garbella and J. H. Wendorff, Makromol. Chem. Rapid Commun. **7**, 591 (1986).
[45]E. A. Jordan, R. C. Ball, A. M. Donald, L. J. Fetters, R. A. L. Jones, and J. Klein (unpublished).
[46]See, for example, Y. Termonia and Z. Alexandrowicz, Mol. Phys. **39**, 725 (1980).